

Geodinamica Acta

ISSN: 0985-3111 (Print) 1778-3593 (Online) Journal homepage: https://www.tandfonline.com/loi/tgda20

An extensional and transtensional origin of elongated magmatic domes and localised transfer faults in the northern Menderes metamorphic core complex, western Turkey

Fuat Erkül, Sibel Tatar Erkül, Hatice Seval Manap & Cihan Çolak

To cite this article: Fuat Erkül, Sibel Tatar Erkül, Hatice Seval Manap & Cihan Çolak (2017) An extensional and transtensional origin of elongated magmatic domes and localised transfer faults in the northern Menderes metamorphic core complex, western Turkey, Geodinamica Acta, 29:1, 139-159, DOI: 10.1080/09853111.2017.1343523

To link to this article: https://doi.org/10.1080/09853111.2017.1343523

© 2017 The Author(s). Published by Informa UK Limited, trading as Taylor & Francis Group

Published online: 03 Jul 2017.

Submit your article to this journal

Article views: 1665

View related articles

View Crossmark data

Citing articles: 5 View citing articles

Full Terms & Conditions of access and use can be found at
https://www.tandfonline.com/action/journalInformation?journalCode=tgda21

GEODINAMICA ACTA, 2017
VOL. 29, NO. 1, 139–159
https://doi.org/10.1080/09853111.2017.1343523

Taylor & Francis
Taylor & Francis Group

OPEN ACCESS Check for updates

An extensional and transtensional origin of elongated magmatic domes and localised transfer faults in the northern Menderes metamorphic core complex, western Turkey

Fuat Erkül[a], Sibel Tatar Erkül[b], Hatice Seval Manap[b] and Cihan Çolak[b]

[a]Vocational School of Technical Sciences, Akdeniz University, Antalya, Turkey; [b]Department of Geological Engineering, Akdeniz University, Antalya, Turkey

ABSTRACT

The northern Menderes metamorphic core complex has complex exhumation history and is one of the key localities to investigate the spatial and temporal relationships of extensional and compressional structures. Detachment faults and syn-extensional plutons are linked to a series of antiforms and synforms and the denudation of the northern Menderes Massif occurred in three stages. The first stage is related to the development of detachment faults under the consistent NE–SW-directed extension. The second stage is represented by a series of elongated magmatic domes that were oriented parallel, oblique and perpendicular to the regional extension direction. Emplacement of these asymmetrical magmatic domes appears to have been controlled by heterogeneous extension and post-dates the extensional Simav detachment fault. On the third stage, progressive heterogeneous extension that led to updoming of plutons has been finally accommodated by a localised and short-lived transfer zone, which was described as the Gerni shear zone for the first time in this study. The transfer zone is formed by a NE-striking, dextral ductile/brittle shear zone that accommodated the propagation of folds, conjugated strike-slip faults and normal- and oblique-slip faults. Mylonites associated with the transfer zone are related to the localisation of strain along the thermally weakened strike-slip fault systems by short-lived intrusions rather than to the development of regional-scale detachment faults. These structures are consistent with a transtensional simple shear model, which properly explains the evolution of extensional and compressional structures exposed in the northern Menderes core complex. Structural setting of the Eğrigöz region is somewhat similar to that of the NE-trending gneiss domes in the northern Menderes Massif and updoming of magma during late stages of detachment faulting appears to have played an important role in the exhumation of lower and upper plate rocks.

ARTICLE HISTORY
Received 11 August 2016
Accepted 14 June 2017

KEYWORDS
Heterogeneous extension; transfer fault; magmatic gneiss dome; simple shear model; extensional detachment

1. Introduction

Metamorphic core complexes (MCC) or gneiss domes commonly exhibit antiformal dome-shaped culminations of deep crustal rocks (Eskola, 1948; Teyssier & Whitney, 2002; Yin, 2004). These domes are widely accompanied by synkinematic migmatitic and magmatic cores and their origin has been explained by various mechanisms involving diapiric flow (Fletcher, 1972; Ramberg, 1981; Teyssier & Whitney, 2002; Verner et al., 2014) and structural control under constrictional or extensional settings (Coney, 1980; Kisters, Vietze, & Buick, 2013; Mancktelow & Pavlis, 1994; Rey, Teyssier, Kruckenberg, & Whitney, 2011; Yin, 1991, 2004). Diapiric flow is regarded as a result of rapid decompression melting of lower and middle crust, while structural culminations in the upper crustal levels are mainly controlled by compressional, strike-slip and extensional tectonic regimes (Vigneresse & Clemens, 2000).

Particularly, elongated and domal geometries of core complexes are caused by extensional detachment faults that extensively occur together with syn-extensional plutons, folds and strike-slip fault systems (Coney, 1980; Crittenden, Coney, & Davis, 1978; Faulds & Varga, 1998; Lister & Baldwin, 1993; Malavieille, 1987; Platt, Behr, & Cooper, 2015; Wernicke & Axen, 1988; Wernicke, Axen, & Snow, 1988; Yin et al., 1999). Antiformal and synformal structures in core complexes may have axes oriented normal, oblique and perpendicular to extension direction (Jolivet, Rimmele, Oberhänsli, Goffe, & Candan, 2004; Martínez-Martínez, Soto, & Balanyá, 2002; Singleton, 2012). Origin of folding in the detachment faults and their respective footwalls has been explained by various mechanisms involving syn-extensional plutonism, pure extension and horizontal compression coupled with horizontal extension (see review by Martínez-Martínez et al. (2002) and references therein). Strike-slip

CONTACT Fuat Erkül fuaterkul@gmail.com

© 2017 The Author(s). Published by Informa UK Limited, trading as Taylor & Francis Group.
This is an Open Access article distributed under the terms of the Creative Commons Attribution License (http://creativecommons.org/licenses/by/4.0/), which permits unrestricted use, distribution, and reproduction in any medium, provided the original work is properly cited.

faults, accommodation zones and transfer zones are accepted as a result of heterogeneous distribution of strain (Faulds & Varga, 1998) and may be spatially and temporally linked to elongated domes and folds in the immediate footwall and hanging-wall units of the core complexes (Fossen, Teyssier, & Whitney, 2013; Malavieille, 1987; Martínez-Martínez, 2006; Martínez-Martínez, Soto, & Balanyá, 2004). Crustal-scale transfer faults may border elongated gneiss domes (Martínez-Martínez, 2006) and accommodate differential stretching between MCCs, as observed in the Cycladic and Menderes core complexes (Le Pourhiet, Huet, May, Labrousse, & Jolivet, 2012; Ring, Laws, & Bernet, 1999).

Syn-extensional plutons intrude as diapirs into the immediate footwall rocks in many cases and occur in different stages of detachment faulting (Campbell-Stone, John, Foster, Geissman, & Livaccari, 2000; Foster & Fanning, 1997; Foster, Schafer, Fanning, & Hyndman, 2001; Lee & Lister, 1992; Lister & Baldwin, 1993). It is a matter of debate whether magmatism in the core of gneiss domes is the cause or driving mechanism of the differential uplift and denudation of footwall rocks (Acocella & Rossetti, 2002; Buck, 1988; Corti et al., 2003; Lister & Baldwin, 1993; Wernicke, 1981). It is known from analogue models and the correlated natural examples that the final shape of shallow-seated plutons is mainly defined by deformation (Castro, 1987; Montanari et al., 2010; Román-Berdiel, 1999; Román-Berdiel et al., 2000; Vigneresse & Clemens, 2000). However, studies that document the detachment-related plutonic activity through detailed structural analysis of brittle faults and folds are rather rare. It is also not clear how detachment faulting has been structurally influenced by the pluton emplacement and what controls the elongation of shallow-seated magmatic domes in the core complex setting.

The Menderes MCC is one of the key localities to investigate the temporal and spatial relationships of syn-extensional plutons, ductile shear zones, brittle faults and folds to better understand the evolution of continental core complexes (Figure 1). In this paper, we provide geological and structural data from the Koyunoba and Eğrigöz plutons and the surrounding units, aimed at deciphering the development of elongated magmatic domes in the northern Menderes MCC. In this study, three tectonic stages have been distinguished associated with the formation of elongated magmatic domes, which are closely linked to the transfer zones that accommodated the extensional and transtensional domains. Microstructural studies on the mylonitic rocks have also been performed to investigate the deformation conditions associated with the transfer zones. Available data from folds and ductile/brittle faults allowed us to discuss the relative timing of major structural elements and to compare the pre-existing geochronological data with our field-based results.

2. Geological setting

Basement units hosting the Koyunoba and Eğrigöz granite plutons comprise the Menderes Massif and the Dağardı Mélange, which were conventionally described as lower and upper plate units, respectively (Thomson & Ring, 2006) (Figure 2). The lower and upper plate units separated by the Simav detachment fault (SDF) were claimed to form the northern margin of the Menderes Massif. The overwhelming multi-scale structural and geochronological data from SDF have already been provided by Işık and Tekeli (2001), Işık, Seyitoğlu, and Çemen (2003), Işık, Tekeli, and Seyitoğlu (2004), Ring and Collins (2005) and Thomson and Ring (2006) (Table 1). SDF has been defined by mylonitic footwall rocks with a top-to-NE sense of shear and the brittlely deformed low-grade rocks above detachment fault. Normal faults and ductile shear zones exposed on the granitic plutons in the northern Menderes Massif also point out a consistent top-to-the N- and NE-directed extension (Erkül, 2010; Ersoy, Helvacı, & Sözbilir, 2010; Işık et al., 2004; Ring & Collins, 2005).

The Menderes Massif in the Eğrigöz region consists of variably deformed Precambrian-Cambrian orthogneisses, metapegmatoids, mica schists and minor marble intercalations, which were formerly described as the Simav metamorphic sequence (Akdeniz & Konak, 1979). Metagranites are slight to moderately foliated and display intrusive contact with the Menderes metamorphic rocks, having similar attitudes of foliation to each other. Although the tectonic setting of the metagranites is not fully understood, U–Pb zircon crystallisation age of 30.04 ± .56 Ma from metagranites suggests their emplacement prior to detachment faulting (Hasözbek, Akay, Erdogan, Satır, & Siebel, 2010). The Dağardı Mélange is part of the İzmir-Ankara Zone and consists of slightly metamorphosed mudstones, shales and sandstones, which form the matrix of recrystallised limestone olistoliths (Akay, Işintek, Erdoğan, & Hasözbek, 2011; Okay, 1989). All these basement units together with granitic plutons were unconformably overlain by a volcano-sedimentary succession that comprises intercalations of thick fluvial and volcaniclastic deposits. Volcaniclastic rocks mainly consist of more than 400-metres-thick ignimbrites and ash fall deposits, which are dominant in the upper parts of the succession in the north-western part of the Eğrigöz and Koyunoba plutons (Figure 2).

Syn-extensional plutons in the northern Menderes Massif are variable in size and display irregular map patterns and rhomb-shaped geometry. The Koyunoba pluton is a NE–SW-elongated (20 × 6 km) dome-shaped body that is intruded into the mica schists, orthogneisses and the Dağardı Mélange (Dora, 1970) (Figures 2, 3). The outermost parts of the Koyunoba pluton are characterised by a-metre-thick cataclastic rocks that include NE- and NW-striking, gently dipping normal faults

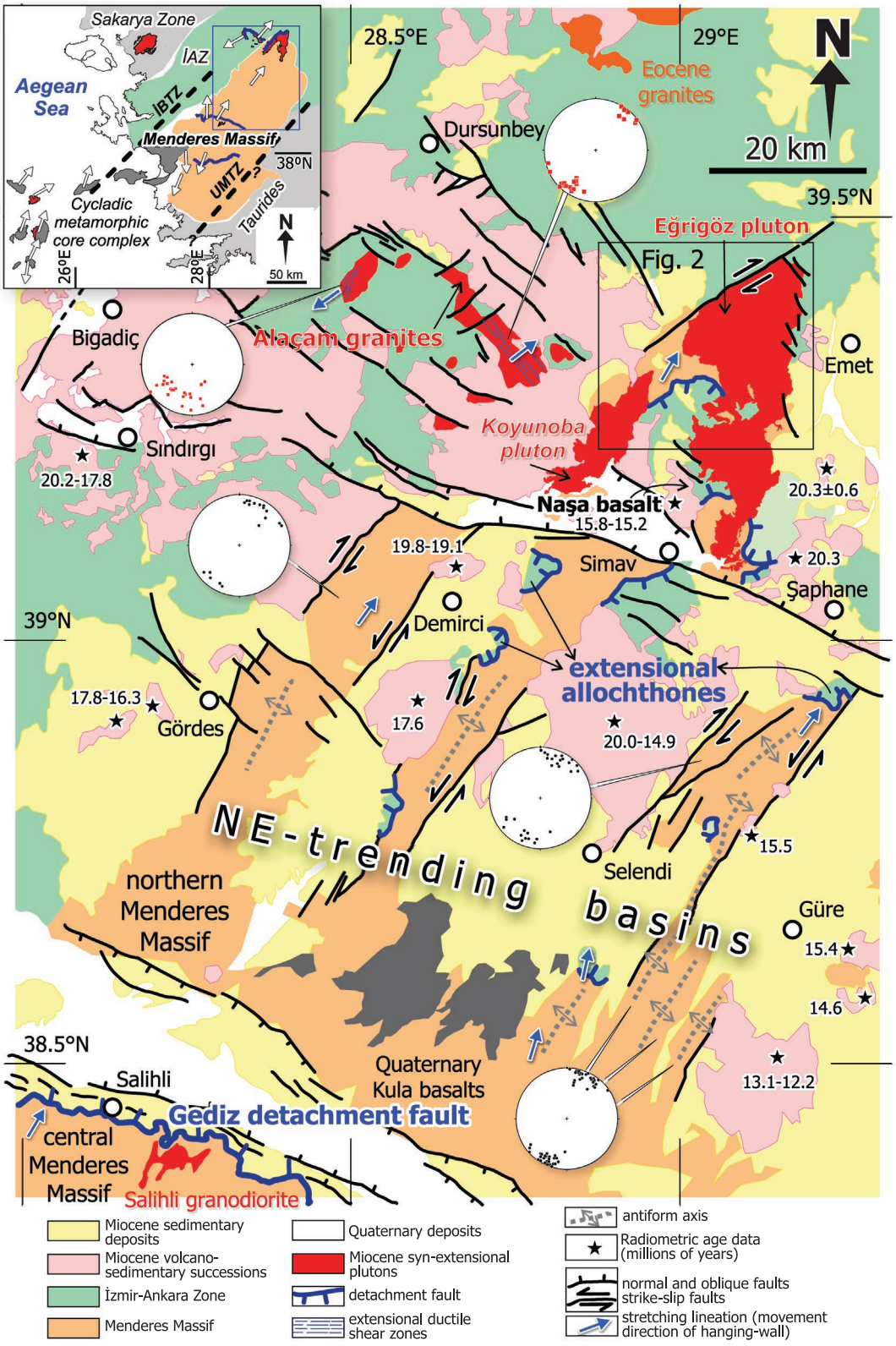


Figure 1. Generalised geological map of western Turkey, including major rock units and structural elements. The inset shows the simplified tectonic map of the Aegean region including major tectonic units of western Turkey. Structural elements were adopted from Yılmaz et al. (2000), Erkül et al. (2005), Çemen, Catlos, Göğüş, and Özerdem (2006), Thomson and Ring (2006), Ersoy et al. (2010), Öner and Dilek (2011), Karaoğlu and Helvacı (2012), Ersoy, Çemen, Helvacı, and Billor (2014) and our own data. Compiled age data of volcanic units are from Ersoy et al. (2014). Lower hemisphere equal-area stereographic projections of lineation patterns measured from footwall rocks of the Menderes Massif (black circle) and mylonitic rocks in the syn-extensional plutons (red square). İBTZ: İzmir-Balıkesir transfer zone. UMTZ: Uşak-Muğla transfer zone.

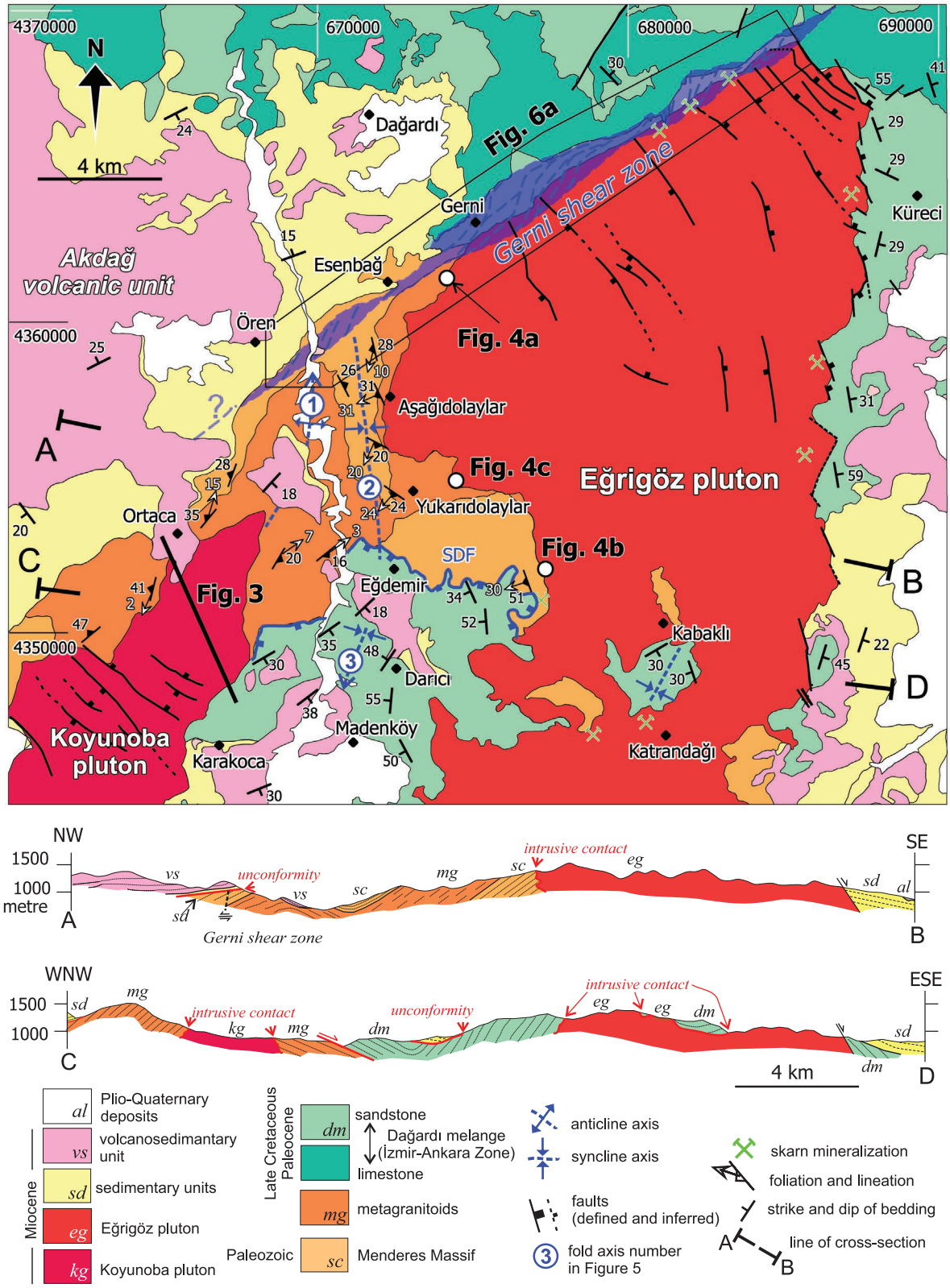


Figure 2. Geological map of the Eğrigöz region. Map coordinates are Universal Transverse Mercator (UTM) grid system. Boundaries of rock units are after Akdeniz and Konak (1979). Numbers in blue circles refer to fold data shown in Figure 5. Location of the Simav detachment fault (SDF) was partly adopted from Ring and Collins (2005).

(Figure 3(a)–(c)). Unconformable contact between the Koyunoba pluton and the overlying Miocene volcanogenic sedimentary rocks is well exposed around Ortaca (Figure 2). The overlying deposits consist of fluvial rocks with imbricated granite boulders and ash fall deposits, from bottom to top. It can be noted that the Miocene deposits are lacking deformational structures associated with low-angle faulting.

The Eğrigöz pluton is about N–S-elongated (40 × 15 km) granite body and can be classified as the largest pluton with its aerial extent of about 330 km^2. It is characterised by equigranular and minor porphyritic granites

Table 1. Summary of geochronological data from the extensional Simav detachment, syn-extensional plutons and surrounding basin deposits associated with the northern Menderes Metamorphic Core Complex.

Lithology	Method	Mineral	Age (Ma)	References
Simav detachment-related rocks				
Mylonitic rocks beneath the detachment	Ar–Ar	Muscovite	22.86 ± .47	Işık et al. (2004)
Orthogneisses of the footwall rocks	Th–Pb ion microprobe	Monazite in garnet porphyroclasts	29.6 ± 1.1 27.9 ± 1.0	Catlos and Çemen (2005)
Migmatites beneath the detachment	U–Th–Pb	Monazite	22.2 ± .2	Cenki-Tok et al. (2015)
Mylonitic rocks associated with the detachment	Ar–Ar Rb–Sr	Muscovite Green/brown biotites	25.5 to 19.8 30 to 8	Bozkurt et al. (2011)
Syn-extensional plutons				
Koyunoba pluton				
Undeformed granite	SIMS U–Th–Pb	Zircon	21.0 ± .2	Ring and Collins (2005)
	U–Pb	Zircon	21.7 ± 1.0	Hasözbek et al. (2010)
	Ar–Ar	Biotite	20.4 ± .1	Altunkaynak et al. (2012)
	U–Pb *in situ* ion microprobe	Zircon	23.2 ± .1–21.1 ± 2.1	Catlos et al. (2012)
	Ar–Ar	Biotite	20.6 ± .5	Çoban et al. (2012)
Eğrigöz pluton				
Undeformed granite	U–Pb Shrimp	Zircon	19.48 ± .29	Altunkaynak et al. (2012)
	Ar–Ar	Hornblende	19.0 ± .1	
		Biotite	18.9 ± .1	
	U–Pb	Zircon	19.4 ± 4.4	Hasözbek et al. (2010)
	Rb–Sr	Biotite	18.77 ± .19	
	SIMS U–Th–Pb	Zircon	20.7 ± .6	Ring and Collins (2005)
	Ar–Ar	Biotie	20.19 ± .28	Işık et al. (2004)
	U–Pb *in situ* ion microprobe	Zircon	20.5 ± 1.1–18.9 ± 1.2	Catlos et al. (2012)
Alaçam granites				
Undeformed granite	U–Pb Shrimp	Zircon	22.60 ± .77	Altunkaynak et al. (2012)
	Ar–Ar	Biotite	20.3 ± .1	
	U–Pb *in situ* ion microprobe	Zircon	23.0 ± 1.8–20.6 ± 1.0	Catlos et al. (2012)
	K–Ar	Biotite	20.9 ± .5–19.9 ± .7	Bingöl, Delaloye, and Ataman (1982)
	Ar–Ar	Biotite	19.87 ± .1–19.5 ± .1	Erkül (2010)
Mylonitised granite	Ar–Ar	Biotite	19.8 ± .1	
Undeformed granite	U–Pb	Zircon	20.3 ± 3.3	Hasözbek et al. (2010)
	Rb–Sr	Biotite	20.01 ± .2–20.17 ± .2	
Surrounding volcanic deposits				
Dacite/rhyolite (West of Koyunoba pluton)	Ar–Ar	Biotite	19.7 ± .5	Çoban et al. (2012)
Dacite/rhyolite (East of Koyunoba pluton)	Ar–Ar	Biotite	19.4 ± .5	
Rhyolite (southeast of the Eğrigöz pluton)	Ar–Ar	Biotite, sanidine	19.82 ± .07–18.04 ± .02	Semiz et al. (2015)

locally enveloped by microgranites and granite porphyries. Leucocratic dykes on the periphery and structurally upper parts of the pluton are rather common. Northern contact of the pluton is formed by mylonites, brittle faults and local occurrences of hornfelsic rocks associated with the clastic rocks of the Dağardı Mélange. Distinct hydrothermal alteration, skarn occurrences and conjugated oblique- and strike-slip faults occur along the eastern contact of the pluton. In contrast, the western contact of the Eğrigöz pluton is intrusive into orthogneisses and metagranites with sharp contact (Figure 4(a)–(c)). Metagranites differ from the intruding equigranular Eğrigöz granites by the presence of slight to intense foliation and tourmaline crystals and the absence of mafic enclaves and hornblende crystals. The roof pendants of the Menderes Massif and Dağardı Mélange within the Eğrigöz pluton include Fe-rich skarn zones with garnet, pyroxene and epidote crystals (Oyman, Özgenç, Tokçaer, & Akbulut, 2013). All aforementioned data indicate that the Eğrigöz and Koyunoba plutons were intruded into the Menderes Massif and the structurally overlying Dağardı Mélange, which is consistent with the observation of Hasözbek et al. (2010).

The Alaçam granites located to the west of the Eğrigöz and Koyunoba plutons comprise a number of elongated domes. The largest pluton reaches up to 19 km long and 5 km wide and its long axis is oriented NW–SE in direction. Detailed information on the Alaçam granites has already been provided by Erkül (2010). The largest pluton has sharp contact with mica schists and includes low-grade extensional ductile shear zones within its inner parts. Ductile shear zones are gently dipping and are mainly comprised of protomylonites that display kinematic indicators of σ-type porphyroclasts, oblique shear bands to main foliation and mica fish structures, indicating a NE–SW-directed extension and top-to-the NE sense of shear. Erkül (2010) indicated that the ductility-deformed quartz and mica and brittlely deformed feldspar and amphibole crystals within the Alaçam granite suggest low-grade deformation conditions at about

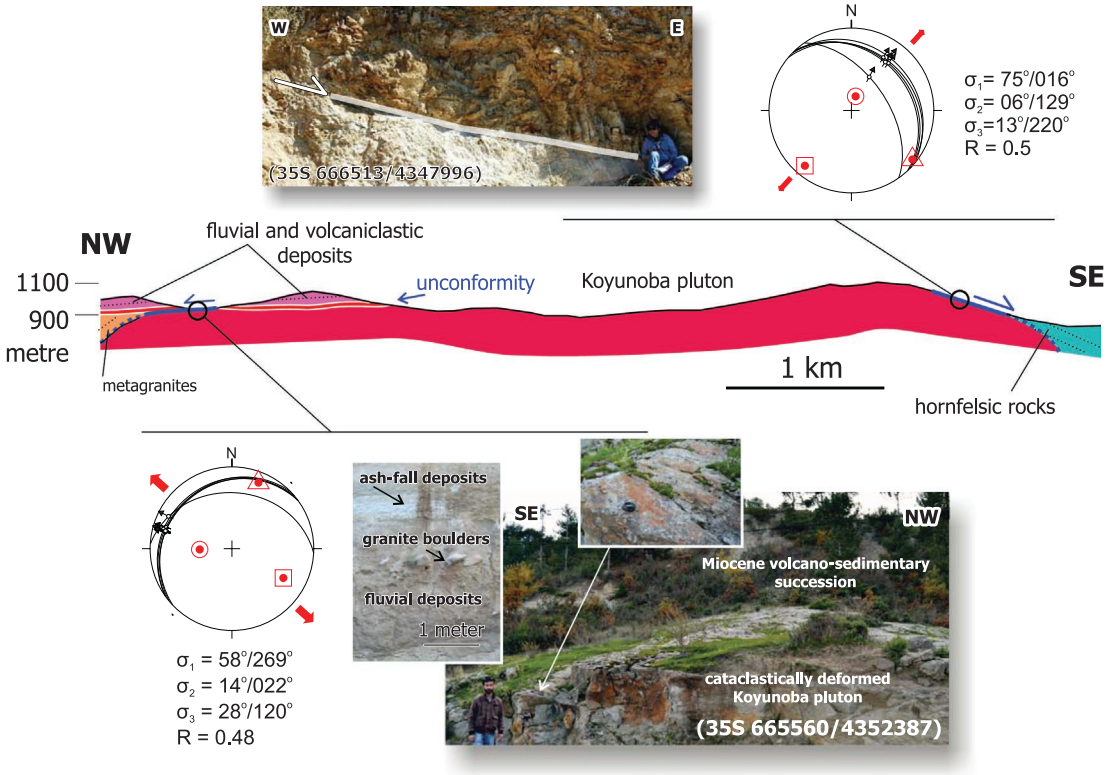


Figure 3. A geological cross section showing structural characteristics of the Koyunoba pluton and the surrounding units. Western contact of the pluton with metagranites is formed by microgranites and leucocratic dykes. Intrusive contact on the eastern margin of the Koyunoba pluton is sharp with hornfelsic clastic rocks of the Dağardı Mélange. Low-angle brittle faults and associated cataclastic rocks occur on the western and eastern margins of the Koyunoba pluton. Note that the Miocene fluvial and volcaniclastic rocks of the Akdağ volcanic unit overlie the low-angle brittle faults. See Figure 2 for location of the cross section.

300–500 °C. Progressive deformation of porphyritic granites together with late-phase felsic dykes is also characteristic, suggesting their syn-tectonic emplacement. Ar–Ar cooling age of 19.8 Ma from the mylonitic rocks within the Alaçam pluton corresponds to the timing of the shearing event.

A summary of geochronological data from the detachment-related rocks, syn-extensional plutons and the volcanic units in the northern margin of the Menderes Massif is presented in Table 1. Radiometric ages associated with SDF range from about 30 to 15 Ma while syn-extensional plutons yielded crystallisation and cooling ages around 21 to 18 Ma.

3. Methods

Existing geological maps, Shuttle Radar Topography Mission (SRTM30) elevation data and NASA MRSID Landsat data were interpreted before conducting field work. All geological and structural data were compiled using GIS software. Standard geological and structural field techniques were applied on the structural elements associated with synextensional plutons and surroundings. Structural methods included systematic measurements of tabular and linear structures.

A total of 151 fault planes with slip line and slip sense have been measured from 17 sites within the plutons and associated shear zones (Table 2). Paleostress tensors and stress inversion calculations were done using the Win Tensor software (Delvaux & Sperner, 2003). The theoretical background for calculations used in the software is based on Wallace (1951), Bott (1959) and Angelier (1989, 1994). During the fault-slip data analyses, carefully examined data from each site were correlated with those from other sites such that the slip data with the same order of occurrence have been grouped together for preliminary stress inversion processing. Stress tensor measurements obtained from the palaeostress analysis are reported on the structural map with stress distribution.

4. Results

The structural elements consist of a series of folds, mylonites and brittle faults (Figure 2). Folds having gently plunging axes were identified by the attitudes of foliation and bedding planes forming the Menderes Massif and the clastic rocks of the Dağardı Mélange (Figure 5). Lineation patterns on the fold limbs formed by the Menderes Massif and the slightly deformed rocks of the Dağardı Mélange trend in N–S to N90°E and plunge at angles between 1° and 47° with an average of 20° towards NE and SW (Figure 5). Mylonites are confined to the northern contact of the Eğrigöz pluton (Figures 6(a)–(d) and 7(a)–(i)). Brittle faults are well exposed on the

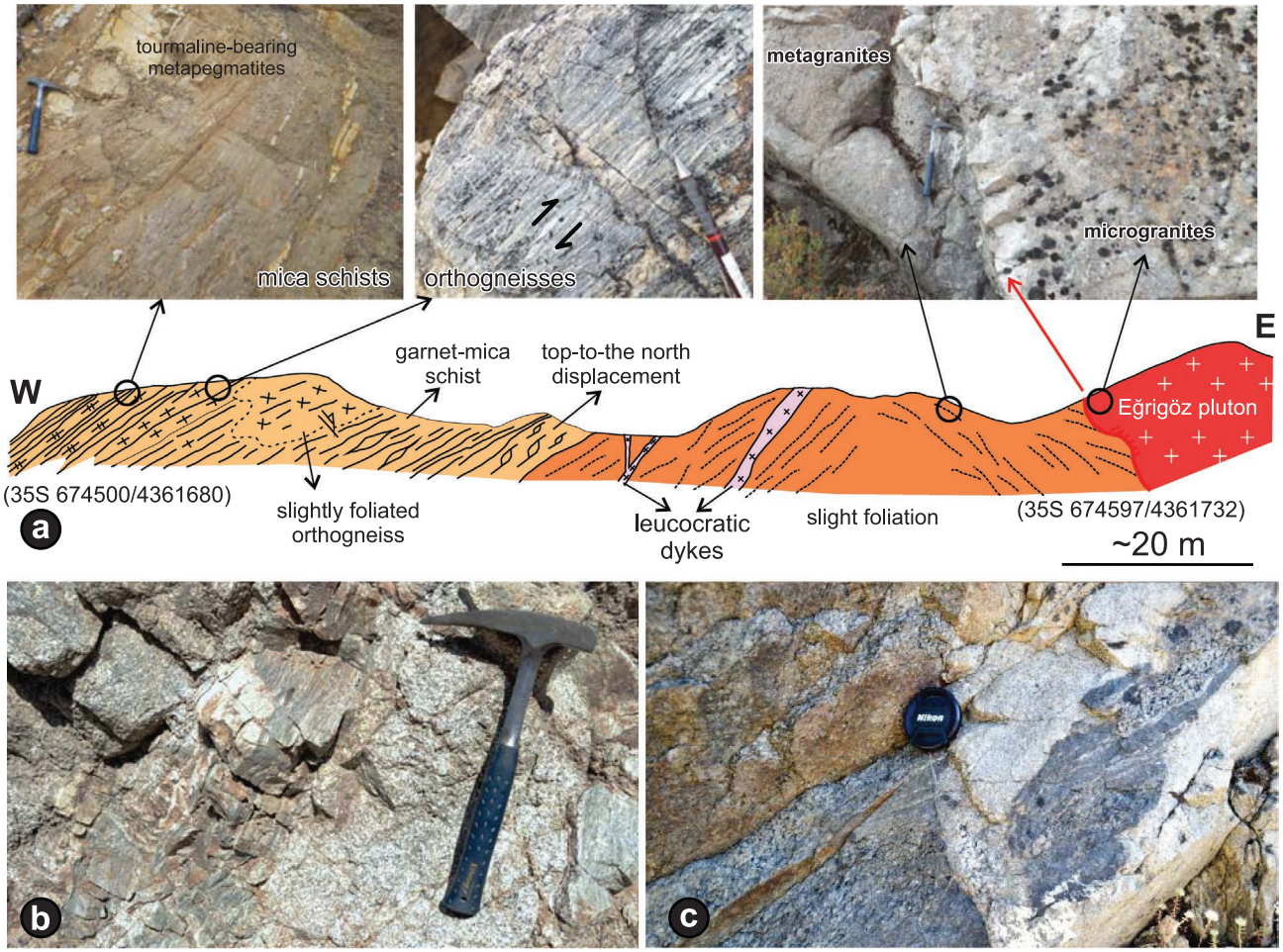


Figure 4. (a) A geological cross section showing lithological characteristics of the metamorphic rocks forming the Menderes Massif and their contact relationship with the Eğrigöz pluton. Metagranites, augen orthogneisses, garnet mica schists and metapegmatoids are structurally alternated to the north-east of Esenbağ. A top-to-the-NE sense of mylonitic shear on the moderately SE-dipping foliation plane is clearly identified within the asymmetric porphyroclasts of orthogneisses and boudined quartz ribbons of the mica schists. Towards the western contact of the Eğrigöz pluton, metagranites are intruded by a few tens of centimeters wide and almost undeformed leucogranitic dykes. Note the cooling contraction joints within the microgranitic margin of the Eğrigöz pluton at the sharp contact with metagranite, suggesting that the metagranitic host rock was cold during emplacement of the pluton. (b) Assimilated orthogneiss within the equigranular granite of the Eğrigöz pluton. (c) Sharp contact between metagranites and the intruding Eğrigöz pluton that includes a host rock fragment. See Figure 2 for location of figures.

Table 2. Stress tensor results of brittle faults measured from plutons and surrounding units.

		σ_1		σ_2		σ_3				
*Site	*N*	plunge	azimuth	plunge	azimuth	plunge	azimuth	**R	R′	Reg
Gerni shear zone										
3	8	27	208	61	4	10	112	.51	1.49	SS
4	8	2	42	86	279	4	132	.50	1.50	SS
6	5	39	150	51	325	2	58	.53	1.47	SS
18	9	1	153	85	249	5	63	.50	1.50	SS
19	5	45	317	43	157	10	57	.41	.41	NS
20	9	29	149	59	307	9	53	.50	1.50	SS
Eğrigöz pluton										
Northern and central parts										
1	11	46	280	38	135	18	30	.40	.40	NS
2	7	73	252	13	109	10	17	.48	.48	NF
8	10	59	152	31	330	1	60	.50	.50	NF
21	16	79	97	8	318	7	227	.66	.66	NF
26	10	70	269	15	130	13	36	.81	.81	NF
Eastern part										
10	16	1	172	77	78	1	263	.82	1.18	SS
13	4	20	353	69	156	6	261	.50	1.50	SS
14	6	28	304	62	122	1	214	.34	1.66	SS
16	7	81	204	5	326	8	57	.46	.46	NF
Koyunoba pluton										
29	7	77	301	13	101	5	192	.50	.50	NF
30	13	79	300	10	95	4	186	.50	.50	NF

*Refer Figure 2 for location of sites. *N*: number of data used in the site; σ_1, σ_2, σ_3: maximum, intermediate and minimum compressive stress axes; *R*: stress ratio; *R*′: stress regime index; Reg: stress regime; NS: normal strike-slip, NF: normal fault, SS: strike-slip;

**R has values ranging between 0 and 1 (Angelier, 1989, 1994). In normal-slip extension, where σ_1 is vertical, radial and pure extension is expressed by $0 < R < .25$ and $.25 < R < .75$, respectively. When σ_1 or σ_2 is vertical, transtensional displacement has R values between .75 and 1. R ratio for pure strike-slip displacement ranges between .25 and .75, where σ_2 is vertical. The stress regime index R' defined by Delvaux et al. (1997) has values of .25–.75 for pure extension, 1.25–1.75 for pure strike-slip and 2.25–2.75 for pure compression.

Eğrigöz and Koyunoba plutons and their surrounding units. All these structures are overlain by an almost undeformed Miocene volcano-sedimentary succession.

4.1. Folds

A series of antiforms and synforms in the Eğrigöz region have been identified by the analysis of attitudes of foliation and bedding planes from the Menderes units and the clastic rocks of the Dağardı Mélange. They have curvilinear, doubly plunging axes almost parallel to each other. Antiform axes appear to extend along the long axis of the Koyunoba and Eğrigöz plutons. One of these, a 15-km-long antiform has an axis oriented parallel to the trend of the Koyunoba pluton (Fold 1 in Figures 2 and 5). Fold limbs strike more or less parallel to the contact of the Koyunoba pluton, forming a NE-trending-elongated dome structure. They dip gently to moderately (16°–55°) and show a slightly asymmetrical antiformal structure with subhorizontal hinge line (Figure 5; Stereoplot 1). The antiform axis trends N42°E and plunges towards NE at an angle of 3°. It can be noted that the foliation planes in the northern part of the Koyunoba pluton dominantly dip northward, while flanks on the outermost central part of the pluton have southward dipping foliation planes, showing a doubly plunging antiform geometry. Northeastern tip of the antiform is abruptly terminated at the Gerni shear zone. It is also marked that the trend of antiform axis and attitudes of stretching mineral lineations within the rock units of the Menderes Massif are oriented almost parallel to the elongation of Koyunoba pluton.

A synform that has almost parallel hinge line was identified to the east of the above-mentioned antiform (Figure 2, Folds 2 and 3). The axis of the synform is about 14 km long and extends over the rock units of the Menderes Massif and the Dağardı Mélange between the Koyunoba and Eğrigöz plutons. It has a doubly plunging and arched axis towards NW (azimuth 354°) and SW (azimuth 196°) (Figure 5, Stereoplots 2 and 3). Northerly plunging synform axis extends across the metagranites and the structurally alternated mica schists. Limbs of northerly plunging synform dip 16–48° and the calculated plunge of π-axis is 4° (Figure 5; Stereoplot 2). Southerly plunging synform has more or less symmetrical, gently dipping limbs formed by the clastic rocks of the Dağardı Mélange (Figure 5; Stereoplot 3). The plunge of π-axis of the synform is 22° towards SW, which is relatively steeper with respect to those of other folds. The elongated dome structure in the Koyunoba pluton is somewhat better differentiated with respect to that of the Eğrigöz pluton. But, it is distinctive that the foliation and bedding planes of the host rocks dip outward the western and eastern contacts of the Eğrigöz pluton, indicating that an antiform occurs to the east of a series of folds described above. The plunge of π-axis of the inferred antiform is 6° towards the south (Figure 5; Stereoplot 4). The calculated axial plane strikes N02°E, which is consistent with the orientation of the long axis of Eğrigöz pluton that forms

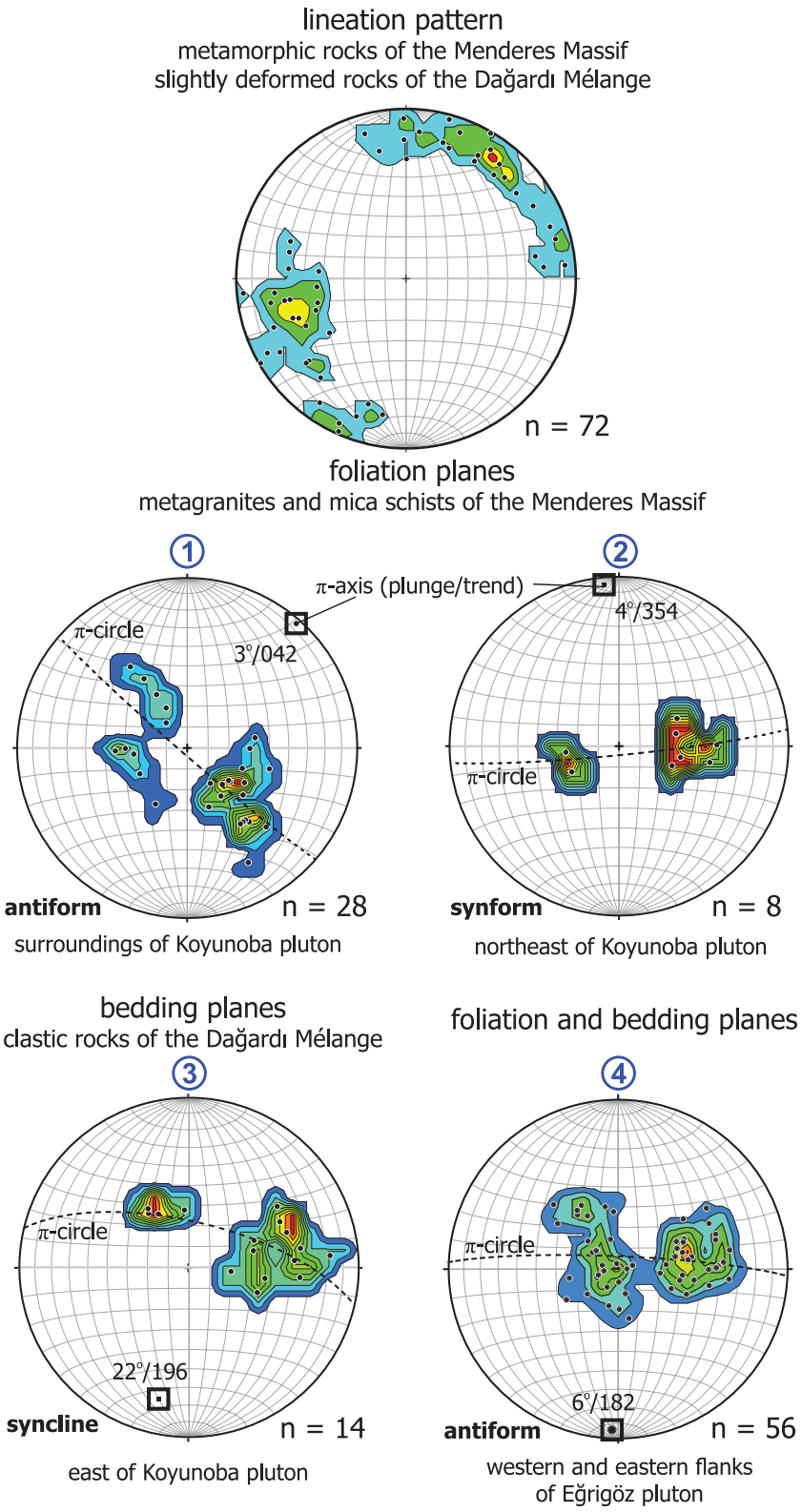


Figure 5. Lower hemisphere equal-area stereographic projections of lineation patterns and pole to foliation and bedding planes measured from lower and upper plate rocks. Density contour plots indicate the percent of data per 1% area. Grid interval is 10°. *n*: number of measurements (black dots on stereoplots). Each contour interval, starting from 0%, is 2% per 1% area. Location of stereoplots 1, 2, 3 and 4 is shown in Figure 2.

the core of the antiform. Almost symmetrical syncline within the roof pendant rocks of the Dağardı Mélange may be regarded as another map-scale evidence for the presence of a ~N–S directed antiform or elongated dome structure along the Eğrigöz pluton (Figure 2).

4.2. The Gerni shear zone

The Gerni shear zone is at least 20 km long, up to 1 km wide and about N65°E-striking tabular structure. It juxtaposes the Dağardı Mélange and the Eğrigöz pluton and

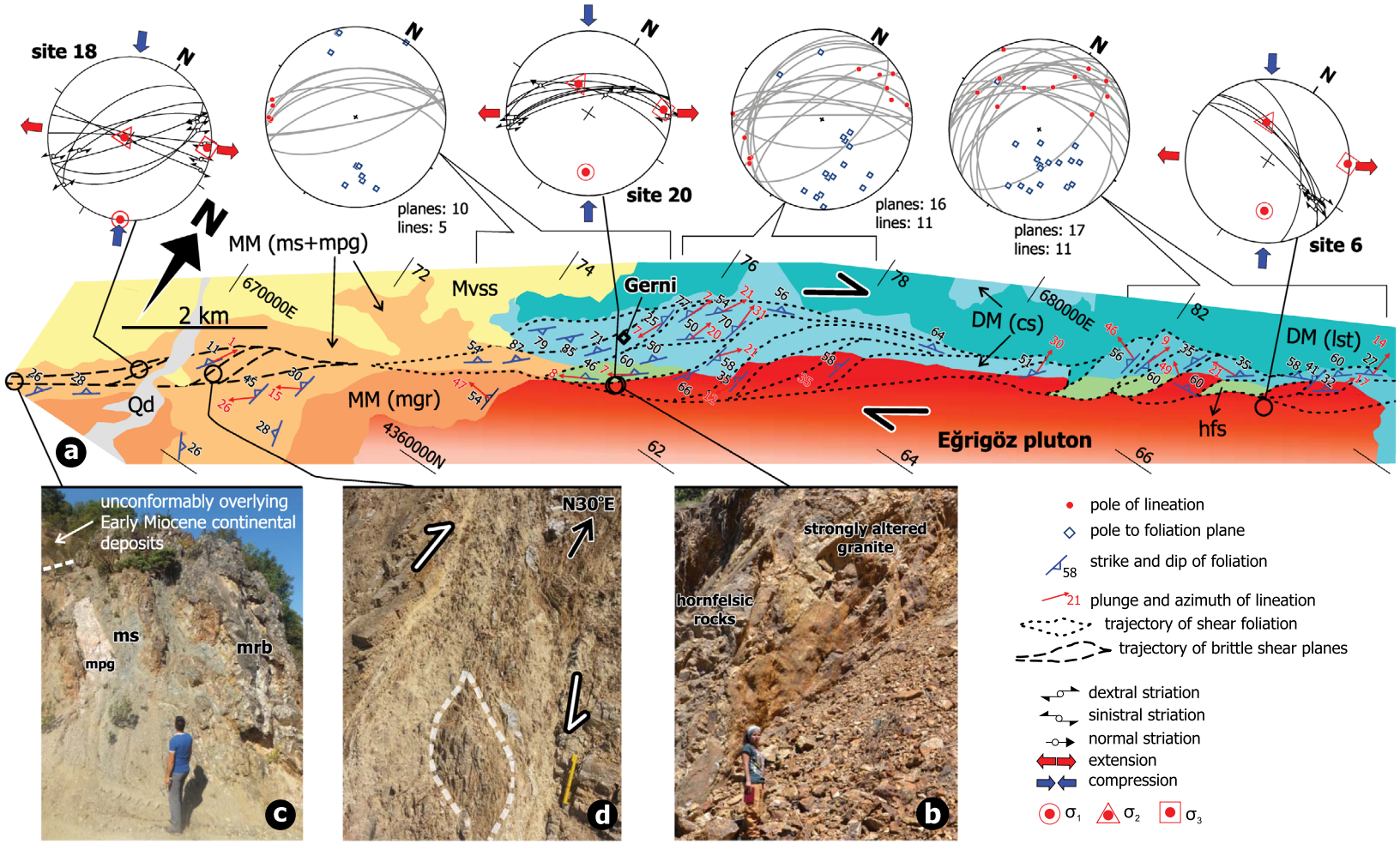


Figure 6. (a) Detailed structural map of the Gerni shear zone north of the Eğrigöz pluton including stereoplots of foliation/lineation data from the mylonitic shear zone and the overprinting brittle fault sets. Refer to Figure 2 for location of fault sites. (b) Brittlely deformed contact zone between the Eğrigöz granite and the hornfels mylonites. (c) Strongly brecciated metamorphic slices of the Menderes Massif within the Gerni shear zone, which is unconformably overlain by thick Miocene fluvial sedimentary sequence belonging to the basal parts of the Akdağ volcanic unit. The view is looking towards the north-east. (d) A mesoscopic-scale dextral shear zone associated with the Gerni shear zone, which cut the mica schists of the Menderes Massif. Outcrop view is subhorizontal to the surface ground. hfs: hornfels, ms: mica-schist, mrb: marble, MM: Menderes Massif, mgr: metagranite, ms: mica schist, mpg: metapegmatoids, DM: Dağardı Mélange, cs: clastic sediments, lst: recrystallised limestone, Mvss: Miocene volcano-sedimentary succession, Qd: Quaternary deposits.

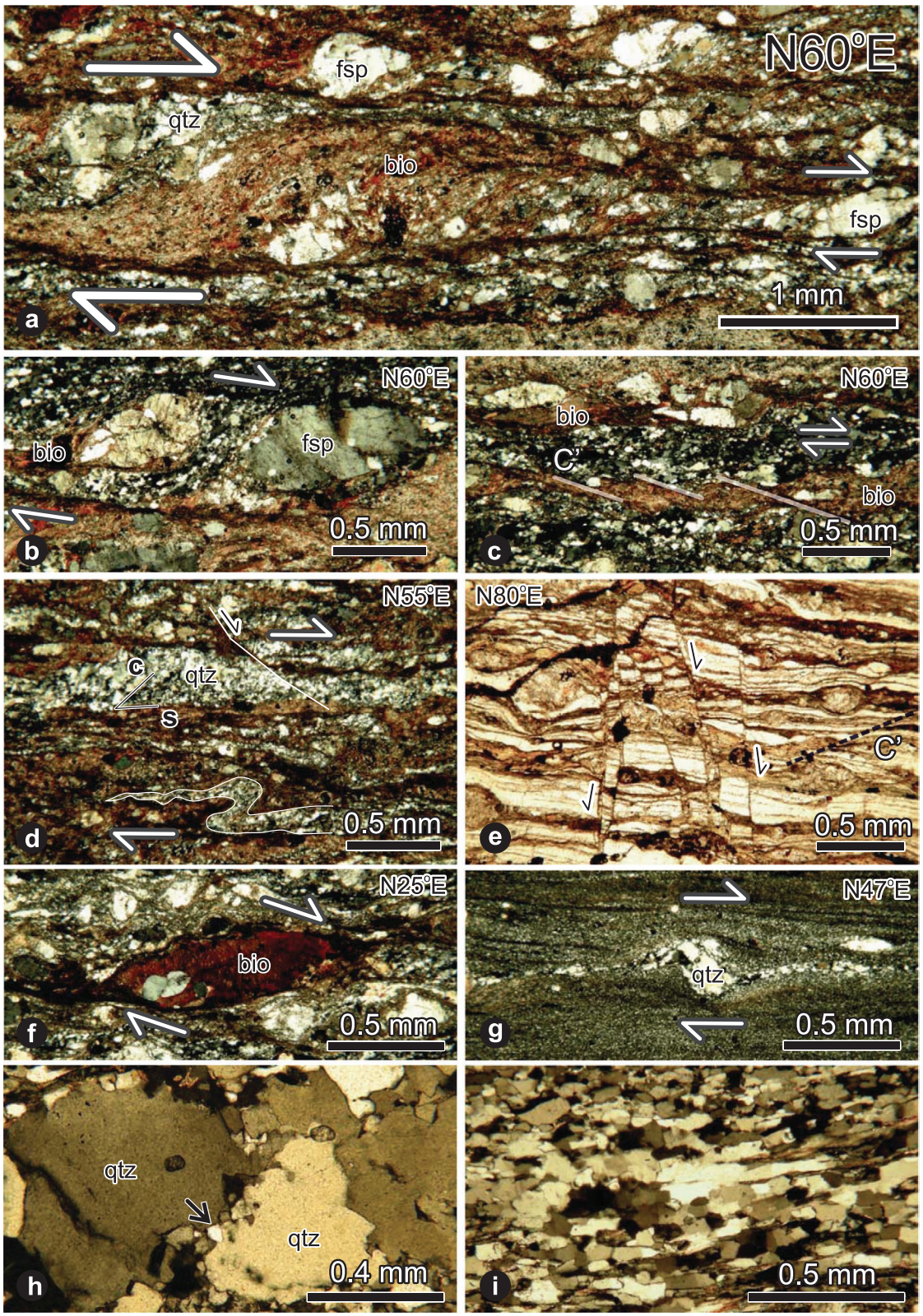


Figure 7. Photomicrographs of granite mylonites and ultramylonites forming the Gerni shear zone. (a) S–C-type shear bands and asymmetrical feldspar porphyroclasts. S-planes are defined by smeared out biotite and sericite trails oblique to the C-planes. Note the similarity of deformation patterns outlined by trajectory of foliation planes to those plotted on the structural map in Figure 6(a). (b) Mantled porphyroclasts enclosed by biotite trails and obliquely oriented, dynamically recrystallised quartz grains. (c) C′-type shear bands well defined by truncated biotite ribbons. (d) Oblique quartz grain-shape foliation and isoclinal folds in quartz aggregates. (e) Microfaults with normal component overprinting the mylonitic foliation. (f) A truncated biotite fish confined between C′-type shear planes. (g) A brittlely fractured, relatively large δ-type quartz porphyroclast with stair stepping in ultramylonites. (h) Bulging recrystallisation (BLG) of quartz grains in granite mylonites (i) Polycrystalline quartz grains formed by subgrain rotation recrystallisation (SGR). All kinematic indicators display normal-dextral shear sense. Crossed polarised light except for Figure 7(e). Sections are parallel to the mineral lineation and normal to the foliation. qtz: quartz, bio: biotite, fsp: feldspar.

also extends within the Menderes Massif (Figure 6(a)). North-eastern sector of the zone includes ductile and the overprinting brittle faults mainly identified within the Eğrigöz pluton with intense alteration and skarn occurrences along the contact zone, while only brittle faults occur in the south-eastern sector. Mylonites are well developed between the clastic rocks of the Dağardı Mélange and equigranular granites together with their hypabyssal equivalents and hornfelsic contact zones. South-western sector is defined by brittle fault clusters extending within the metapegmatoids and mica schists and is formed by fault breccia zones that are comprised of variably sized and strongly deformed metapegmatoids and mica schists (Figure 6(b)). The fault zone is unconformably overlain by fluvial and boulder-bearing conglomerates that form the basal sedimentary units below the Akdağ volcanic unit. Brittlely sheared mica schists display a dextral shear sense (Figure 6(c)). Subordinate brittle shear zones are obliquely oriented to the main trajectory of shear zone boundary. The overprinting brittle fault sets, which are dominantly NE–SW in direction, are well exposed along the contact zone that consists of mylonitised granites, hornfelsic rocks and sandstones of the Dağardı Mélange (Figure 6(d)).

4.3. Mylonites

Mylonites are located in the NE part of the Gerni shear zone and are exposed within 10 km long and up to one km wide area along the intrusive contact zone between the Eğrigöz pluton and the Dağardı Mélange (Figures 2, 6(a)). They are formed by shearing of equigranular granites and microgranites of the Eğrigöz pluton, hornfelses and clastic rocks of the Dağardı Mélange. Foliation planes in mylonites dominantly strike NE in direction, but N- and NW-striking planes also occur. Their dip is mainly towards NW and ranges between 12 and 85°. Lineation patterns in the south-west of the shear zone plunge subhorizontally (4–8°) towards NE and SW while the north-eastern part is characterised by variable foliation and lineation attitudes (Figure 6(a)). Foliation planes are mainly formed by sericite and minor chlorite bands and the mineral stretching lineation is distinguished by elongated quartz grains at outcrop scale.

Microstructures and kinematic indicators are relatively well identified in granite mylonites that can be classified as protomylonites and minor ultramylonites. Protomylonites are defined by feldspar porphyroclasts surrounded by smaller, recrystallised quartz grains and mica flakes formed by biotite, sericite and minor chlorite crystals. S-C-type shear bands are formed by obliquely oriented, smeared out biotite and sericite crystals together with dynamically recrystallised quartz grains, surrounding the asymmetrical *σ*-type feldspar porphyroclasts (Figure 7(a)). Dynamically recrystallised quartz grains mainly occur as elongated crystals with c-axis oblique to main foliation (Figure 7(b)). Undulose extinction and brittle fractures are rather common in mantled porphyroclasts of older quartz and feldspar crystals within granites. Quartz grains around the *σ*-type porphyroclasts are relatively fine-grained and sutured together with mica grains while larger quartz subgrains form ribbons almost parallel to the foliation planes. These ribbons are commonly displaced with C′-type shear bands and locally include isoclinal microfolds (Figure 7(c), (d)). Protomylonites are locally overprinted by steeply dipping microfaults that display normal shear sense and are locally filled by late-stage mica crystals (Figure 7(e)). Truncated biotite fishes were also identified between C′-type shear bands (Figure 7(f)). Ultramylonites locally occur within the protomylonites and are characterised by lacking or small porphyroclasts and alternation of mica and quartz ribbons. Minor δ-type quartz porphyroclasts within very fine-grained ultramylonites show stair stepping (Figure 7(g)). Asymmetrical structures of mantled porphyroclasts, S–C- and C′-type shear bands, biotite fish and oblique grain-shape foliation in quartz ribbons indicate a normal-dextral sense of shear. Quartz ribbons within the mylonites were formed by relatively smaller quartz grains that display grain boundaries related to bulging recrystallisation (BLG) to subgrain rotation (SGR), suggesting relatively low-grade plastic deformation conditions (Figure 7(h), (i)).

4.4. Brittle faults

Low-angle brittle faults were identified on the structurally marginal parts of the Koyunoba pluton (Figure 3(a)). They occur within the equigranular granites that are intensely brecciated around fault planes. Any significant alteration or evidence of fluid circulation has not been recorded associated with low-angle brittle faults. In the western part of the pluton, they strike NE–SW in direction and dip towards NW at an angle of 18–32° (Figure 3(b)). Another low-angle fault set located to the east of the Koyunoba pluton strikes NW–SE and dips NE at angles of 22–30°. Slickenlines on these faults indicates dip-slip displacement (Figure 3(c)).

High-angle faults associated with the Gerni shear zone are dominated by strike-slip fault clusters. Fault planes are steeply dipping (>50°), locally vertical and display dextral and sinistral displacements (Figure 8(a)). The high-angle faults are well exposed in the marginal parts of the Eğrigöz pluton and hornfelsic host rocks (Figure 6(b)). To the south-west of the zone, fault clusters juxtapose the strongly brecciated slices of mica schist, metapegmatoids and marbles belonging to the Menderes Massif (Figure 6(c)). Dextral shear within the mica-schists can be observed at outcrop scale (Figure 6(d)).

North-eastern and eastern margins of the Eğrigöz pluton are characterised by NW- and NE-striking synthetic and antithetic fault clusters. The NW-striking normal

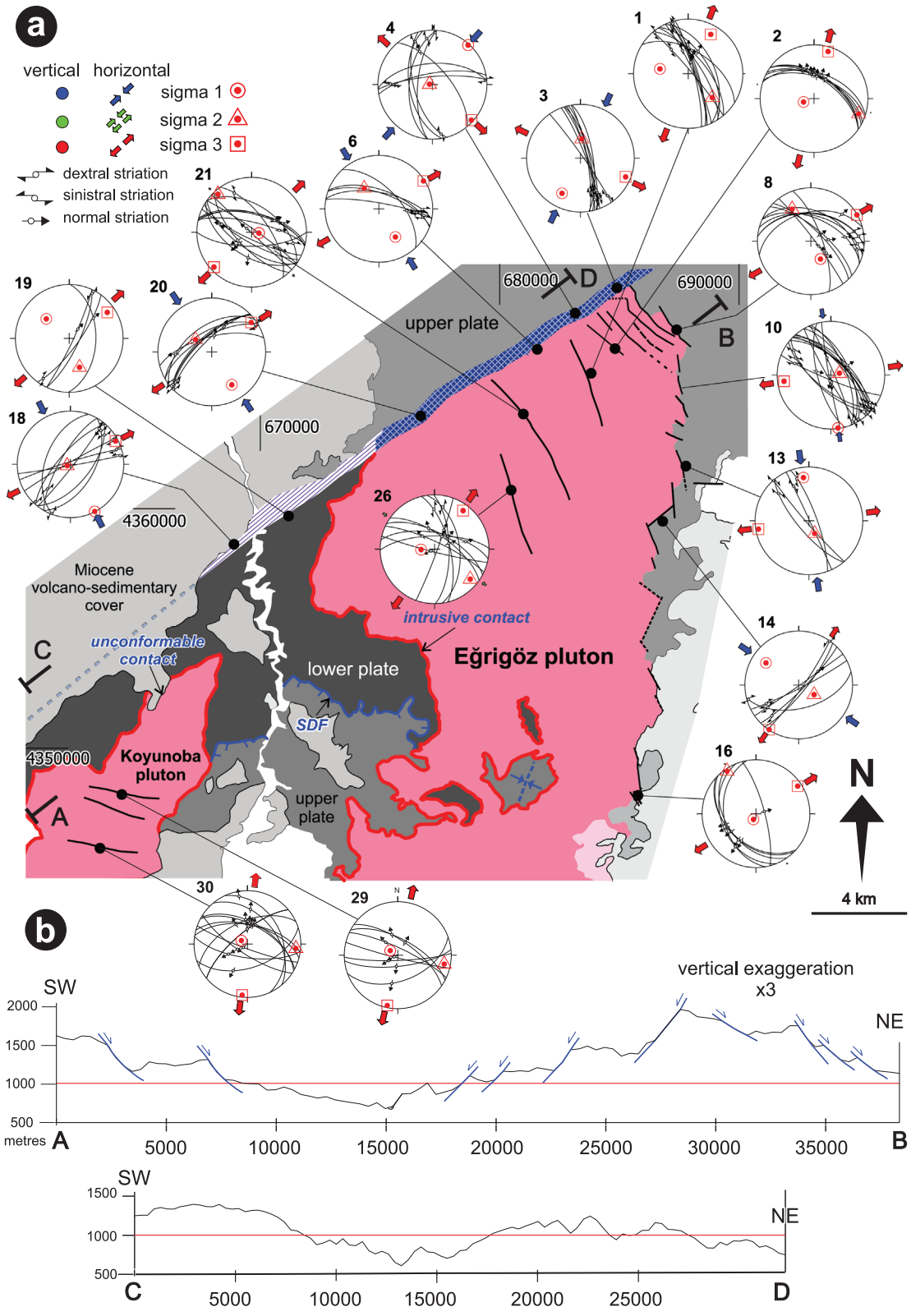


Figure 8. (a) Schmidt lower hemisphere equal-area projections of fault-slip data and principal stress directions from brittle faults in the Eğrigöz region. Refer to Table 2 for fault-slip measurements. Numbers on the upper left of stereoplots correspond to fault site number. (b) Topographic profiles parallel to the strike of the Gerni shear zone.

faults occur in the central parts of the Eğrigöz pluton, and the north-eastern tip of the pluton is mainly dominated by NW-striking and NE-dipping normal faults (Figure 8(a)). Eastern margin consists of a series of NNW- and NE-striking oblique- and strike-slip faults, but pure strike-slip displacement is observed in NNW-striking faults dipping at angles of 40–90°. High-angle normal faults exposed within the central parts of the Koyunoba pluton strike variably, but dominantly NW–SE and W–E in directions. They consist of conjugated sets of normal and oblique faults dipping moderately to steeply at angles of 35–84° (Figure 8(a)).

4.5. Paleostress analysis

Paleostress orientations are compatible with dominant strike-slip, oblique strike-slip and normal-slip components with vertical and subvertical σ_1 and σ_2 together with consistent NE- and minor NW-trending σ_3 stress axes (Figure 8(a), Table 2). Fault-slip data have been measured from the strike-slip faults with minor oblique- and dip-slip components, which overprinted the mylonitic rocks within the Gerni shear zone. The stress distribution computed from these fault sets is dominated by vertical and subvertical σ_2 coupled with subhorizontal σ_1 and σ_3, which trend in NW–SE and NE–SW (Figure 8(a), sites 3, 4, 18 and 20). Moderately plunging σ_1 and σ_2 axes in sites 6 and 19 also occur but display similar paleostress tensors to other sites. The stress distribution of fault sets from the northern, central and eastern parts of the Eğrigöz pluton is mainly characterised by subhorizontal and consistently NE-trending σ_3 axes (Figure 8(a); Table 2). Fault sets within the northern and central parts of the Eğrigöz pluton have dominantly subvertical σ_1, while fault sets in the eastern margin have subvertical σ_2 axes, indicating a coupling of NE–SW extension with NW–SE compression (Figure 8(a)). NW- and NE-striking-conjugated fault sets with oblique-slip displacement together with the minor dip-slip component within the Koyunoba pluton are characterised by subvertical σ_1 and NNE-trending σ_3 axis. Comparison of stress tensor results indicates that the minimum compressional stress axes have similar orientations while the orientation of maximum and intermediate stress axes differs significantly.

Paleostress analysis of fault slickenlines from all fault sites indicates pure strike-slip to the pure extensional regime with computed R and R' values of .34–.82 and .40–1.66, respectively (Table 2). Stress tensor results computed from brittle faults within the Gerni shear zone are remarkably contrasting and define two distinct deformation patterns: (1) Strike-slip dominated deformation under NW–SE extension and NE–SW compression (fault sites 3 and 4) (Figure 8(a)). Calculated R' values 1.49–1.50 are consistent with the pure strike-slip regime (Table 2). (2) NE- and NW-striking faults showing NE–SW extension coupled with NW–SE compression (fault sites 6, 18–20). This pattern has similar R and R' values (R = .50–.53 and R' = 1.47–1.50) to first deformation pattern but differs with stress axis orientations. Coupling of the strike- and oblique-slip fault sets is consistent with the transtensional regime as indicated by R' values between .41 and 1.50. The central and eastern parts of the Eğrigöz pluton have stress tensor results consistent with almost pure NE–SW-directed extension. R and R' values ranging between .5 and .8 indicate a normal and oblique faulting together with the minor strike-slip regime. The eastern margin of the Eğrigöz pluton is dominated by the strike- and oblique-slip faults having calculated R and R' values of .34–.82 and .44–1.66, respectively. All these results reveal that the strike-slip component has been predominant under NE–SW-trending extension. Stress tensor results calculated from fault-slip data within the Koyunoba pluton yielded NNE-SSW-directed extension, showing slight deviation in stress orientations measured from fault sites around the Eğrigöz pluton. Computed R and R' values of .50 from two sites indicate normal slip displacement.

5. Discussion

5.1. Kinematics of the Gerni shear zone

The Gerni shear zone has been formerly described as a detachment fault, separating the Menderes Massif and the structurally overlying Dağardı Mélange (Işık et al., 2003; Ring & Collins, 2005). The detachment origin on the northern margin of the Eğrigöz pluton has not been previously supported by detailed field evidence and the arguments mainly rely on the interpretation that the metagranites in the footwall rocks are a mylonitic envelope, which progressively grades into undeformed Eğrigöz and Koyunoba plutons towards the structurally inner parts. The volcano-sedimentary succession overlying the mylonitic envelope was regarded as supra-detachment basin deposits. Our observations demonstrate that the mylonitic rocks were intruded by the Eğrigöz plutons and the metagranites were cold during pluton emplacement. Therefore, we argue that the metagranites are genetically unrelated to the detachment faulting and the development of the Gerni shear zone is a result of the post-detachment transtensional event. Reported U–Pb zircon age of 30.04 ± .56 Ma from the metagranites also supports the older origin (Hasözbek et al., 2010).

The Gerni shear zone is unconfined to a zone juxtaposing the footwall and hanging-wall units and also occurs within the Pre-Cambrian mica-schist as a steeply dipping shear clusters. Parallelism on the attitudes of gently plunging stretching lineations and the brittle fault slickenlines developed within steeply dipping mylonites indicate a normal-dextral displacement (Figure 6). Trajectories of steeply dipping mylonites also mark a clear dextral shear sense. Paleostress analysis of brittle faults overprinting the mylonites also confirms that the dextral movement along the fault blocks that was induced by the NE–SW-directed extension coupled with compression. Local extension axis is almost parallel to the common orientation of the shear zone and to the regional extension direction defined by consistent stretching lineation trends in detachment faults and footwall mylonites of the northern Menderes Massif. Parallel or transverse orientation of shear zones and extension direction is in line with the common definition of transfer zone that is formed as a result of heterogeneous strain in extended domains (cf. Gibbs, 1984). Small groups of normal- and oblique-slip faults terminate in the major shear zone, suggesting that the strain is transferred directly from the normal faults into a zone of

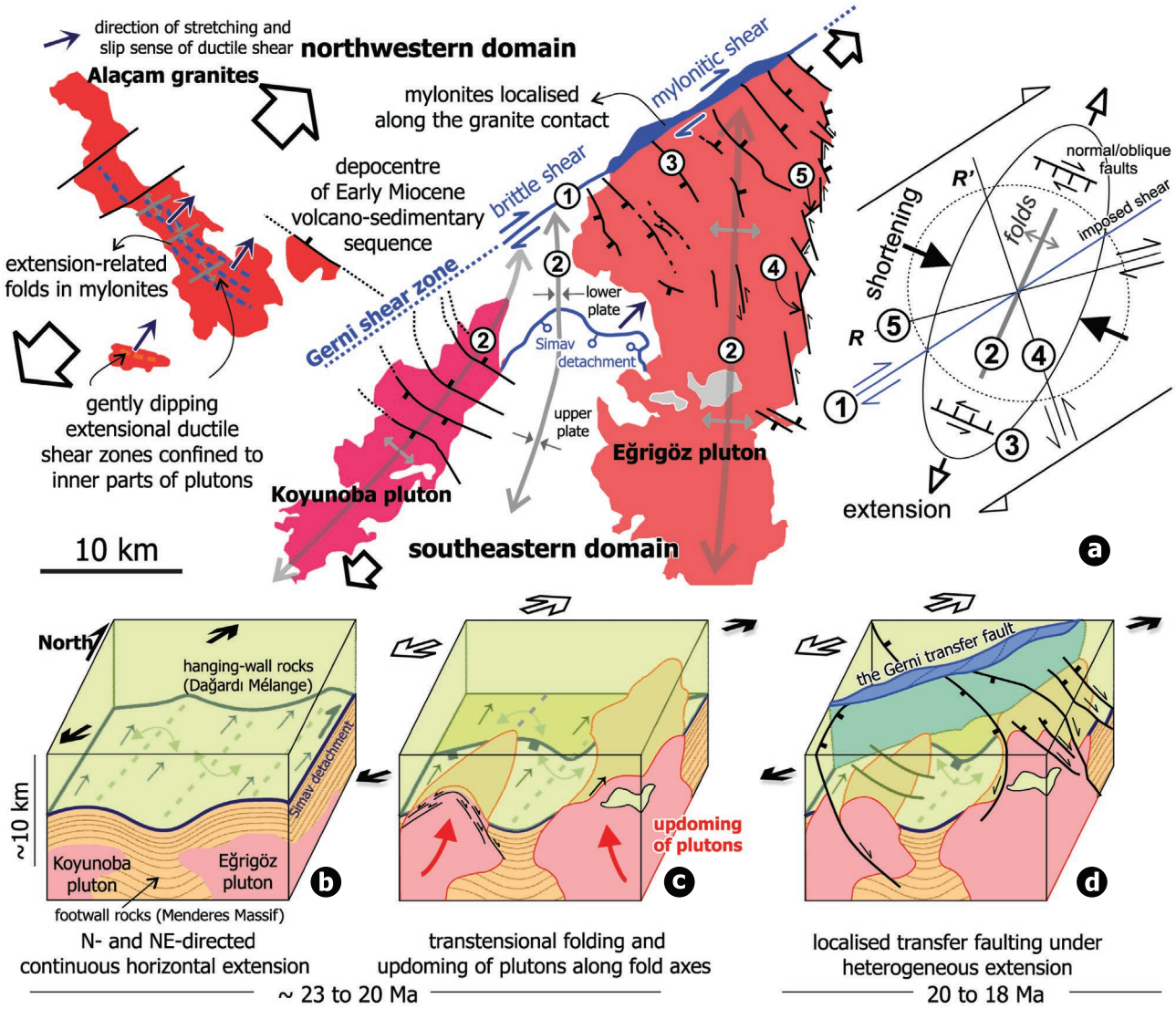


Figure 9. (a) A sketch map summarising the structural elements in two extensional domains separated by the Gerni shear zone in the northern Menderes Massif. The simple shear model has been modified from Waldron (2005). (1) Imposed shear or master fault, (2) folds oblique to the shear direction, (3) normal/oblique-slip faults, (4) synthetic Riedel shear and (5) antithetic Riedel shear. (b–d) A simplified 3D model showing evolutionary model for the major structures described in this study. (b) Early stages of extension caused detachment faulting and folding in the lower and upper plate rocks. (c) Detachment faulting event is followed by updoming of granitoid plutons under the transtensional regime, leading to the development of a series of antiforms with the magmatic core. Low-angle brittle faults formed on the periphery and marginal parts of the plutons were interpreted to have formed during progressive solidification of outer parts of magma above brittle/ductile transition. (d) Ongoing inflation of magma along the hinge lines of antiforms is inferred to have ceased the detachment faulting and initiated the synthetic and antithetic shear zones and transfer zones under the heterogeneous extensional regime.

strike-slip or oblique-slip faults (cf. Faulds & Varga, 1998). Development of transfer fault in the Eğrigöz region is also evidenced by an abrupt topographic change in two extensional domains separated by a structural boundary, lying parallel to the major extension direction, i.e. the Gerni shear zone (Figure 8(b)). The south-eastern domain shows discrete topographic steps controlled by normal- and oblique-slip faults obliquely oriented to major shear zone and display the highest topography. The north-eastern domain displays relatively gentle topography underlain by the Early Miocene sedimentary infill of broad depressions. It can be argued that the basin with abundant coarse clastic sediments at the basal parts may be related to the depression of north-western domain and the uplift of south-eastern domain owing to the differential stretching of extensional domains along the Gerni shear zone.

We demonstrate that the Gerni shear zone forms an abrupt boundary between two extensional domains having variably oriented magmatic domes with different geometries and deformation styles (Figure 9). The NW-trending, elongated Alaçam granite in the north-western domain is comprised of mylonitic rocks within the inner parts of the pluton, having stretching lineations top-to-the NE-sense of shear (Erkül, 2010). This shear sense is parallel to the orientation of the Gerni shear zone and the regional extension direction but perpendicular to the long axis of the pluton. The syn-extensional Alaçam granites strongly resemble elongated plutons emplaced into the upper crust under almost pure extensional conditions (Corti et al., 2003; Le Pourhiet et al., 2012; Román-Berdiel, 1999; Román-Berdiel et al., 2000). Comparison of analogue and natural examples of extensional plutons by Román-Berdiel (1999) showed that the synkinematic intrusions under pure extensional regime are strongly elongated parallel to the major tectonic discontinuities and follow the direction of normal faults. Similar structural patterns were described in the gneiss domes with synkinematic intrusions in Tinos delimited by north and south Cycladic detachment systems, which were interpreted to have been as a result of the NE-directed extension. However, it is notable that these magmatic domes appear to be spatially and temporally linked to strike-slip fault systems (Jolivet et al., 2010; Le Pourhiet et al., 2012). On the other hand, asymmetrical and extension-parallel-elongated Koyunoba and Eğrigöz plutons display distinct deformation patterns to those exposed in the Alaçam granite. When all structural elements correlated with each other, tectonic evolution of the south-eastern domain is in overall agreement with the simple shear model summarised by Waldron (2005), explaining the successive development of folding and faulting patterns in transtensional strike-slip fault systems (Figure 9(a)). In the simple shear model, the Gerni shear zone may be correlated with the dextral major shear that is oblique to fold axes and conjugated strike-slip faults controlled by coupling of horizontal extension and horizontal compression. The orientation of fold axes that lie along the Koyunoba and Eğrigöz plutons is in line with an echelon fold as a result of compressive component normal to a major horizontal extension within a dextral strike-slip shear zone. A striking feature of fold axes is their arched or curved geometry, which may be attributed to the ongoing transtensional shearing event during the folding stage. Conjugated strike-slip faults defined in the eastern part of the Eğrigöz pluton are consistent with antithetic and synthetic Riedel shears. Normal- and oblique-slip faults were also formed perpendicular to the extension component within the dextral shear zone in the region. All these characteristics of the Gerni shear zone support its occurrence as a transfer zone rather than an extensional detachment fault.

5.2. Origin of localised ductile shear zones

A remarkable feature of the mylonitic rocks associated with the Gerni shear zone is their localisation along the contact between the Eğrigöz pluton and the Dağardı Mélange while the other sectors of the shear zone have been solely deformed in a brittle manner. It may be inferred that the Eğrigöz pluton might have been responsible for forming suitable conditions for limited ductile deformation along the contact zone. Microstructural characteristics of mylonites demonstrate that the recrystallised quartz grains within the mylonites display inter-grain relationships typical for bulging and subgrain rotation, corresponding to the deformation temperatures of about 350–500 °C. However, feldspar porphyroclasts display lacking or slight brittle fracturing, suggesting temperature conditions below 500 °C. Such low-grade ductile deformation can be explained by short-lived thermal event caused by the emplacement of the Eğrigöz pluton that may have provided the necessary heat to induce plastic behaviour (cf. (Lister & Baldwin, 1993; Parsons & Thompson, 1993). These mylonites are somewhat comparable to the low-grade extensional ductile shear zones recorded within the inner parts of the Alaçam granites (Erkül, 2010). The brittle overprint on the mylonites might be related to the progressive cooling of the pluton during shearing as the temperature of the intruding pluton was too low to induce ductile deformation. It may be argued that localised ductile shear develops when igneous activity coincides with shearing event; otherwise, shear zone occurs in a brittle manner as clearly observed in the south-western part of the Gerni shear zone. Therefore, we suggest that the mylonites associated with the Gerni shear zone are related to the localisation of strain along the thermally weakened strike-slip fault systems by short-lived igneous intrusions rather than to the development of regional-scale detachment faults. Limited ductile deformation along the marginal and inner parts of the plutons might

have occurred at shallow crustal levels owing to heat transfer by plutons that have been strongly influenced by pure extensional and transtensional regimes.

5.3. Timing of the Gerni shear zone

Geological and structural constraints on the Eğrigöz and Koyunoba plutons point out that they were emplaced at shallow crustal levels. Their shallow emplacement is characterised by the presence of sharp intrusive contacts of the plutons surrounded by the associated leucogranitic hypabyssal intrusions into the country rocks and occurrences of skarn zones. Thomson and Ring (2006) also noted that the near concordance of the apatite (U–Th)/He, zircon fission track and apatite fission track ages with the U–Pb zircon ages from the Eğrigöz and Koyunoba plutons can be regarded as a result of very rapid post-emplacement cooling at a very shallow crustal level and pluton updoming likely ceased the activity of SDF. In contrary, Bozkurt, Satır, & Buğdaycıoğlu (2011) argued for the SDF activity between ca. 30 and 8 Ma. Catlos, Jacob, Oyman, & Sorensen (2012) also claimed the long-term activity of SDF between 30.0 and 14.7 Ma based on U–Pb *in situ* ion microprobe zircon dating of syn-extensional plutons in the northern Menderes Massif. Radiometric ages of around 21 to 19 Ma can be considered as the most likely time interval for the emplacement and cooling of the Eğrigöz and Koyunoba plutons, which is consistent with the arguments of Ring and Collins (2005) based on SIMS U–Pb zircon age data (Table 1). The Eğrigöz and Koyunoba plutons appear to have intruded into the hanging-wall and footwall rocks of SDF dated at about 23 Ma (Cenki-Tok et al., 2015; Işık et al., 2004) and the volcano-sedimentary succession that unconformably overlies the Koyunoba pluton yielded Ar–Ar ages of 19.7 ± .5 and 19.4 ± .5 Ma (Table 1; Çoban, Karacık, & Ece, 2012). Basal parts of the succession include clastic sediments with abundant granite clasts derived from the Koyunoba and Eğrigöz plutons, suggesting that the denudation of syn-extensional granites must have occurred before extensive felsic volcanic activity. These age data indicate that the Eğrigöz and Koyunoba plutons were emplaced after the development of SDF and before deposition of volcano-sedimentary succession.

Crystallisation and cooling ages of the Eğrigöz and Koyunoba plutons and the overlying volcano-sedimentary sequence summarised above can be used to constrain the relative timing of the Gerni shear zone that operated as a localised transfer zone in the northern Menderes Massif. Localisation of the ductile deformation along the margin of the Eğrigöz pluton may be attributed to the coupling of thermal weakening by the heat of a pluton with strain localisation under transtensional setting. The Gerni shear zone must have propagated immediately following the emplacement of the Eğrigöz pluton as evidenced by the occurrences of strongly mylonitic hornfelses along the contact zone. On the other hand, a brittlely deformed south-western sector of the shear zone is unconformably overlain by the undeformed sedimentary sequence with granite boulders and must have terminated its activity prior to deposition of the volcano-sedimentary succession. Hence, U–Pb ages of the Eğrigöz pluton between 20.7 and 19.48 Ma can be accepted as the onset of mylonitic deformation within the Gerni shear zone (Table 1). This age can be correlated with the Ar–Ar biotite age of 19.8 ± .1 Ma from granite protomylonites associated with the Alaçamdağ pluton. These constraints suggest that the shear zone has been active for a very short time period as the Gerni shear zone and the associated plutons were already denudated and eroded into the fault-controlled Miocene depocenters in the Eğrigöz region.

5.4. Regional tectonic implications

During early stages of extension, SDF was accepted to have occurred immediately below ductile/brittle transition, and the lower plate rocks were progressively uplifted as evidenced by brittle deformation over mylonites. SDF has been a major extensional structure in the exhumation of the Menderes Massif and north-eastward translation of upper plate rocks, i.e. İzmir-Ankara Zone, as a consequence of the thinning of continental crust under the crustal-scale, NE–SW-directed extensional regime. One might expect to observe a major N-dipping major detachment fault that separated the upper and lower plate rocks analogous to the Gediz detachment fault in the central Menderes MCC. However, exposures of detachment boundary are largely obscured and discontinuous in the northern Menderes MCC and SDF dipping towards the south-west are confined between the Eğrigöz and Koyunoba plutons. Another significant feature of these exposures is the fact that the folded trajectory of SDF lies along the culmination of doubly plunging synform. Our observations revealed that the trajectory of SDF ends abruptly at the pluton contacts and the lower and upper plates occur as roof pendants within the plutons, suggesting that the propagation of detachment faulting was terminated by pluton emplacement.

Elongated Eğrigöz and Koyunoba granitic domes are separated by a relatively narrow synform that may be attributed to the doming at the core of upright folds developed in the course of a horizontal compression coupled with regional horizontal extension (cf. Castro, 1987; Platt, 1980). Doming or diapiric emplacement of plutons is generally caused by density inversion. Stress distribution having compressive component promotes the rising of less dense magma into the core of antiforms and normal faults may develop along the margins of the dome (Castro, 1987). Low-angle brittle faults confined to the marginal and structurally upper parts of the Koyunoba pluton may be interpreted as a

result of progressive updoming of the pluton as marginal parts solidified rapidly above the brittle-ductile transition in the upper crust. We infer that irregular attitudes of detachment faults may be explained by inflation of magma into an upper crustal level above the ductile/brittle transition. Although it is not clear whether the magmatism has a major role on the warping of detachment faults during early stages of regional extension in western Turkey, magma updoming are closely linked to the late stage folding on the lower and upper plate rocks and warping of detachment faults.

Upper plate rocks in the NE-trending basins exposed over the Menderes Massif occur as extensional allochthons above variably dipping detachment faults having kinematic indicators consistent with the top-to-the-NE sense of shear. Extensional allochthons were located on the limbs or synforms of extension-parallel gneiss domes. Such extensional detachment exposures were relatively well described around Kula (Ersoy et al., 2010), Gördes (Bozkurt et al., 2011) and Uşak-Güre basins (Karaoğlu & Helvacı, 2012) (Figure 1). Structural elements in the NE-trending-elongated gneiss domes in the northern Menderes Massif are rather similar to those exposed in the Eğrigöz region. These domes occur as NE-trending, almost evenly spaced antiformal structures together with synformal depressions that are filled by Miocene deposits and interbedded volcanic units. Volcanic edifices can be accepted as a surface projection of shallow seated and unexposed plutons beneath the gneissic domes in the NE-trending basins. Cross-gradient joint geophysical inversion of gravity and aeromagnetic data from the northern Menderes Massif demonstrated that a series of evenly spaced intrusions on the upper crust occur along the NE-trending broad antiforms and synforms, which may imply the connection of folding with magmatism (Gessner, Gallardo, Wedin, & Sener, 2016). The NE-trending and steeply dipping strike- and oblique-slip faults, which are almost parallel to the direction of extension and fold axes, propagated on the flanks of antiforms and extruded the volcanic units.

We propose that the development of the NE-trending antiforms and synforms in the northern Menderes Massif might have been controlled by a transtensional regime that induced the updoming of the granitic plutons. Moreover, deformation patterns of brittle domains and ductile shear zones within the Eğrigöz and Koyunoba plutons revealed that the NE–SW-directed horizontal extension coupled with compressional component was continuous during magma emplacement. Thomson and Ring (2006) argue that rapid erosion occurred after removal of about 2–3 km of overburden after cessation of SDF activity and before deposition of sedimentary rocks over detachment surface and syn-extensional plutons. We suggest that updoming of plutons along antiform axes terminated the detachment faulting and resulted in uplift and eventually erosion of upper and lower plate rocks. Erosion of topographically elevated domal structures into synforms formed remnants of upper plate rocks occurring as extensional allochthons over the warped detachment surface. It is also worth to emphasise that SDF yielded a wide range of cooling ages commonly ranging between 30 and 15 Ma. Synextensional plutons have overlapping crystallisation and cooling ages between 21.7 and 18.7 Ma and volcanism with post-orogenic affinity lasted until 12.2 Ma, implying broad occurrences of rapidly cooled magma pulses in western Turkey (Karaoğlu & Helvacı, 2012). It must be taken into consideration that a wide range of cooling ages measured from SDF can be alternatively explained by warping and reactivation of an old detachment due to emplacement and updoming of short-lived pulses of magmatic activity (Ring, Johnson, Hetzel, & Gessner, 2003). Lister and Baldwin (1993) demonstrated that the intruding plutons beneath the extensional detachments may provide heat input to initiate short-lived thermal events, leading to pulses of ductile deformation. Therefore, we suggest that a wide range of cooling ages measured from SDF mylonites can be considered as another significant evidence for updoming of plutons in the northern Menderes MCC.

Strike-slip-dominated shear zones bordering the western and eastern margins of the Menderes MCC have been recognised as NE-trending and crustal-scale transfer zones, which lie parallel to the regional extension direction (Brun & Sokoutis, 2010; Gessner et al., 2016; Jolivet et al., 2015; Ring et al., 1999). The shear zones on the western margin are inferred to have been active since Late Cretaceous and are comprised of major NE-trending dextral and sinistral fault sets accompanied by NW- and E–W-trending faults (İzmir-Balıkesir Transfer Zone, (Erkül, Helvacı, & Sözbilir, 2005); İzmir shear zone, (Brun & Sokoutis, 2010); the West Anatolia Transfer Zone, (Gessner, Gallardo, Markwitz, Ring, & Thomson, 2013)). But the tectonic evolution of the zone is still controversial due to multiphase deformational periods, block rotations and complex interactions between core complexes and strike-slip/rift-related faults (Karaoğlu, 2014; Karaoğlu & Erkül, 2015; Ring et al., 1999; Uzel et al., 2015). The eastern margin of the Menderes Massif is bordered by a sinistral shear zone named Uşak-Muğla transfer zone, which is supposed to have acted in a transtensional setting since early middle Miocene (Karaoğlu & Helvacı, 2012, 2014). These transfer zones bordering the Menderes Massif were active during core complex development and accommodated the NE–SW-trending regional extension. We suggest that the tectonic events of folding, pluton updoming and localised transfer zone development in the northern Menderes MCC appear to have been controlled by crustal-scale transfer zones. Contemporaneous development of these structural elements can be well explained by transtensional deformation following the uniform NE-directed extension that caused the development of SDF. The Gerni shear zone marks a localised dextral displacement during Early Miocene under a

heterogeneous extension that caused the development of the NE-trending transfer zones bordering the Menderes MCC.

6. Conclusions

Our field-based data demonstrate that the northern MMCC experienced a complex deformation history that is distinguished by detachment faults, a series of folds with elongated magmatic domes, transfer zones, normal- and oblique-slip faults and conjugated strike-slip faults. Three stages of deformation have been recognised during the evolution of the northern MMCC: (1) development of the Simav detachment fault under consistent NE–SW-directed extension, (2) emplacement and updoming of syn-extensional granitoids under heterogeneous strain accommodating pure extension and transtensional setting and (3) development of the transfer zone, i.e. Gerni shear zone, in response to heterogeneous strain. We suggest that the warping and denudation of SDF are closely linked to the pulses of magmatic activity, occurring as elongated magmatic domes intruded into the lower and upper plate rocks. Updoming of plutons under extensional and transtensional regimes probably uplifted the detachment faults above the brittle-ductile transition. This study also revealed that the ductile shear zones associated with syn-extensional plutons might not be necessarily connected to a regional-scale, i.e. detachment-related, deformation. These zones can be explained by a coupling of strain and thermal pulses of magmatic activity, which can generate local thermal weakening to induce ductile deformation along the pluton contact.

Acknowledgements

The comments on the earlier version of the manuscript by Veysel Işık and Uwe Ring have been gratefully acknowledged. Authors thank Şule Gürboğa and Bozkurt Çiftçi for their help with paleostress analysis. The manuscript was greatly improved through reviews by referees Laurent Jolivet and an anonymous reviewer. Thanks are also due to Erdin Bozkurt for his patience during editorial handling.

Disclosure statement

No potential conflict of interest was reported by the authors.

Funding

This work was supported by Akdeniz University Research Project [grant number 2014.02.0121.023]; TUBİTAK Research Projects [grant numbers 112Y244 and 115Y360].

ORCID

Fuat Erkül http://orcid.org/0000-0002-4918-3042
Sibel Tatar Erkül http://orcid.org/0000-0002-7583-0071
Hatice Seval Manap http://orcid.org/0000-0001-7079-1643
Cihan Çolak http://orcid.org/0000-0002-7167-2918

References

Acocella, V., & Rossetti, F. (2002). The role of extensional tectonics at different crustal levels on granite ascent and emplacement: An example from Tuscany (Italy). *Tectonophysics, 354*, 71–83.

Akay, E., Işintek, I., Erdoğan, B., & Hasözbek, A. (2011). Stratigraphy of the Afyon Zone around Emet (Kütahya, NW Anatolia) and geochemical characteristics of the Triassic volcanism along the northern Menderes Massif. *Neues Jahrbuch für Mineralogie – Abhandlungen, 188*, 297–316.

Akdeniz, N., & Konak, N. (1979). Menderes masifinin Simav dolayındaki kayabirimleri ve metabazik, metaultramafik kayaların konumu. *Türkiye Jeoloji Kurumu Bülteni, 22*, 175–183.

Altunkaynak, Ş., Dilek, Y., Genç, C. Ş., Sunal, G., Gertisser, R., Furnes, H., … Yang, J. (2012). Spatial, temporal and geochemical evolution of Oligo-Miocene granitoid magmatism in western Anatolia, Turkey. *Gondwana Research, 21*, 961–986.

Angelier, J. (1989). From orientation to magnitudes in paleostress determinations using fault slip data. *Journal of Structural Geology, 11*, 37–50.

Angelier, J. (1994). Fault slip analysis and paleostress reconstruction. In P. L. Hancock (Ed.), *Continental deformation* (pp. 53–100). Oxford: Pergamon Press.

Bingöl, E., Delaloye, M., & Ataman, G. (1982). Granitic intrusions in western Anatolia: A contribution to the geodynamic study of this area. *Eclogae Geologicae Helvetiae, 75*, 437–446.

Bott, M. H. P. (1959). The mechanics of oblique slip faulting. *Geological Magazine, 96*, 109–117.

Bozkurt, E., Satır, M., & Buğdaycıoğlu, Ç. (2011). Surprisingly young Rb/Sr ages from the Simav extensional detachment fault zone, northern Menderes Massif, Turkey. *Journal of Geodynamics, 52*, 406–431.

Brun, J.-P., & Sokoutis, D. (2010). 45 m.y. of Aegean crust and mantle flow driven by trench retreat. *Geology, 38*, 815–818.

Buck, W. R. (1988). Flexural rotation of normal faults. *Tectonics, 7*, 959–973.

Campbell-Stone, E., John, B. E., Foster, D. A., Geissman, J. W., & Livaccari, R. F. (2000). Mechanisms for accommodation of Miocene extension: Low-angle normal faulting, magmatism, and secondary breakaway faulting in the southern Sacramento Mountains, southeastern California. *Tectonics, 19*, 566–587.

Castro, A. (1987). On granitoid emplacement and related structures. A review. *Geologische Rundschau, 76*, 101–124.

Catlos, E. J., & Çemen, İ. (2005). Monazite ages and the evolution of the Menderes Massif, western Turkey. *International Journal of Earth Sciences, 94*, 204–217.

Catlos, E. J., Jacob, L., Oyman, T., & Sorensen, S. (2012). Long-term exhumation of an Aegean metamorphic core complex granitoids in the Northern Menderes Massif, western Turkey. *American Journal of Science, 312*, 534–571.

Çemen, İ., Catlos, E. J., Göğüş, O., & Özerdem, C. (2006). Postcollisional extensional tectonics and exhumation of the Menderes massif in the Western Anatolia extended terrane, Turkey. In Y. Dilek (Ed.), *Postcollisional tectonics and magmatism in the Mediterranean region and Asia* (Vol. 409, pp. 353–379). Boulder, Colorado: Geological Society of America Special Paper.

Cenki-Tok, B., Expert, M., Işık, V., Candan, O., Monié, P., & Bruguier, O. (2015). Complete Alpine reworking of the northern Menderes Massif, western Turkey. *International Journal of Earth Sciences, 105*, 1507–1524.

Çoban, H., Karacık, Z., & Ece, Ö. I. (2012). Source contamination and tectonomagmatic signals of overlapping Early to Middle Miocene orogenic magmas associated with shallow

continental subduction and asthenospheric mantle flows in Western Anatolia: A record from Simav (Kütahya) region. *Lithos, 140–141*, 119–141.

Coney, P. J. (1980). Cordilleran metamorphic core complexes. In M. D. Crittenden, P. J. Coney, & G. H. Davis (Eds.), *Cordilleran metamorphic core complexes* (Vol. GSA Memoir 153, pp. 7–34). Boulder: Geological Society of America.

Corti, G., Bonini, M., Conticelli, S., Innocenti, F., Manetti, P., & Sokoutis, D. (2003). Analogue modelling of continental extension: A review focused on the relations between the patterns of deformation and the presence of magma. *Earth-Science Reviews, 63*, 169–247.

Crittenden, M., Coney, P. J., & Davis, G. (1978). Tectonic significance of metamorphic core complexes in the North American Cordillera. *Geology, 6*, 79–80.

Delvaux, D., & Sperner, B. (2003). New aspects of tectonic stress inversion with reference to the TENSOR program. *Geological Society Special Publication, 212*, 75–100.

Delvaux, D., Moeys, R., Stapel, G., Petit, C., Levi, K., Miroshnichenko, A., & … Sankov, V. (1997). Paleostress reconstructions and geodynamics of the Baikal region, Central Asia, Part 2. Cenozoic rifting. *Tectonophysics, 282*, 1–38.

Dora, O. Ö. (1970). Karakoca granit masifinde petrolojik ve metalojenik etütler. *Maden Tetkik Arama Enstitüsü Dergisi, 73*, 10–26.

Erkül, F. (2010). Tectonic significance of synextensional ductile shear zones within the Early Miocene Alacamdağ granites, northwestern Turkey. *Geological Magazine, 147*, 611–637.

Erkül, F., Helvacı, C., & Sözbilir, H. (2005). Evidence for two episodes of volcanism in the Bigadic borate basin and tectonic implications for western Turkey. *Geological Journal, 40*, 545–570.

Ersoy, Y. E., Helvacı, C., & Sözbilir, H. (2010). Tectono-stratigraphic evolution of the NE–SW-trending superimposed Selendi basin: Implications for late Cenozoic crustal extension in Western Anatolia, Turkey. *Tectonophysics, 488*, 210–232.

Ersoy, E. Y., Çemen, İ., Helvacı, C., & Billor, Z. (2014). Tectono-stratigraphy of the Neogene basins in Western Turkey: Implications for tectonic evolution of the Aegean Extended Region. *Tectonophysics, 635*, 33–58.

Eskola, P. E. (1948). The problem of mantled gneiss domes. *Quarterly Journal of the Geological Society, 104*, 461–476.

Faulds, J. E., & Varga, R. J. (1998). The role of accommodation zones and transfer zones in the regional segmentation of extended terranes. *Geological Society of America Special Papers, 323*, 1–45.

Fletcher, R. C. (1972). Application of mathematical model to emplacement of mantled gneiss domes. *American Journal of Science, 7*, 197–216.

Fossen, H., Teyssier, C., & Whitney, D. L. (2013). Transtensional folding. *Journal of Structural Geology, 56*, 89–102.

Foster, D. A., & Fanning, C. M. (1997). Geochronology of the northern Idaho batholith and the Bitterroot metamorphic core complex: Magmatism preceding and contemporaneous with extension. *Geological Society of America Bulletin, 109*, 379–394.

Foster, D. A., Schafer, C., Fanning, C. M., & Hyndman, D. W. (2001). Relationships between crustal partial melting, plutonism, orogeny, and exhumation: Idaho-Bitterroot batholith. *Tectonophysics, 342*, 313–350.

Gessner, K., Gallardo, L. A., Markwitz, V., Ring, U., & Thomson, S. N. (2013). What caused the denudation of the Menderes Massif: Review of crustal evolution, lithosphere structure, and dynamic topography in southwest Turkey. *Gondwana Research, 24*, 243–274.

Gessner, K., Gallardo, L. A., Wedin, F., & Sener, K. (2016). Crustal structure of the northern Menderes Massif, western Turkey, imaged by joint gravity and magnetic inversion. *International Journal of Earth Sciences, 105*, 2133–2148.

Gibbs, A. D. (1984). Structural evolution of extensional basin margins. *Journal – Geological Society (London), 141*, 609–620.

Hasözbek, A., Akay, E., Erdoğan, B., Satır, M., & Siebel, W. (2010). Early Miocene granite formation by detachment tectonics or not? A case study from the northern Menderes Massif (Western Turkey). *Journal of Geodynamics, 50*, 67–80.

Işık, V., & Tekeli, O. (2001). Late orogenic crustal extension in the northern Menderes Massif (western Turkey); Evidence for metamorphic core complex formation. In E. Bozkurt & R. Oberhänsli (Eds.), *Menderes Massif (western Turkey): Structural, metamorphic and magmatic evolution* (Vol. 89, pp. 757–765). Berlin: Springer International.

Işık, V., Seyitoğlu, G., & Çemen, İ. (2003). Ductile-brittle transition along the Alasehir detachment fault and its structural relationship with the Simav detachment fault, Menderes massif, western Turkey. *Tectonophysics, 374*, 1–18.

Işık, V., Tekeli, O., & Seyitoğlu, G. (2004). The $^{40}Ar/^{39}Ar$ age of extensional ductile deformation and granitoid intrusion in the northern Menderes core complex: implications for the initiation of extensional tectonics in western Turkey. *Journal of Asian Earth Sciences, 23*, 555–566.

Jolivet, L., Rimmele, G., Oberhänsli, R., Goffe, B., & Candan, O. (2004). Correlation of syn-orogenic tectonic and metamorphic events in the Cyclades, the Lycian nappes and the Menderes massif. Geodynamic implications. *Bulletin de la Societe Geologique de France, 175*, 217–238.

Jolivet, L., Lecomte, E., Huet, B., Denèle, Y., Lacombe, O., Labrousse, L., … Mehl, C. (2010). The North Cycladic detachment system. *Earth and Planetary Science Letters, 289*, 87–104.

Jolivet, L., Menant, A., Sternai, P., Rabillard, A., Arbaret, L., Augier, R., … Le Pourhiet, L. (2015). The geological signature of a slab tear below the Aegean. *Tectonophysics, 659*, 166–182.

Karaoğlu, Ö. (2014). Tectonic controls on the Yamanlar volcano and Yuntdagi volcanic region, western Turkey: Implications for an incremental deformation. *Journal of Volcanology and Geothermal Research, 274*, 16–33.

Karaoğlu, Ö., & Erkül, F. (2015). Comment on 'Paleomagnetic evidence for an inverse rotation history of Western Anatolia during the exhumation of Menderes core complex' by Uzel et al. (Earth Planet. Sci. Lett. 415 (2015) 108–125). *Earth and Planetary Science Letters, 427*, 309–311.

Karaoğlu, Ö., & Helvacı, C. (2012). Structural evolution of the Uşak-Güre supra-detachment basin during Miocene extensional denudation in western Turkey. *Journal of the Geological Society, 169*, 627–642.

Karaoğlu, Ö., & Helvacı, C. (2014). Isotopic evidence for a transition from subduction to slab-tear related volcanism in western Anatolia, Turkey. *Lithos, 192–195*, 226–239.

Kisters, A. F. M., Vietze, M. E., & Buick, I. (2013). Deformation and age of the Stinkbank Pluton and implications for the correlation of tectonometamorphic episodes in the Pan-African Damara Belt. *South African Journal of Geology, 115*, 309–326.

Le Pourhiet, L., Huet, B., May, D. A., Labrousse, L., & Jolivet, L. (2012). Kinematic interpretation of the 3D shapes of metamorphic core complexes. *Geochemistry, Geophysics, Geosystems, 13*, 1–17.

Lee, J., & Lister, G. S. (1992). Late Miocene ductile extension and detachment faulting, Mykonos, Greece. *Geology, 20*, 121–124.

Lister, G. S., & Baldwin, S. L. (1993). Plutonism and the origin of metamorphic core complexes. *Geology, 21*, 607–610.

Malavieille, J. (1987). Extensional shearing deformation and kilometer-scale 'a' – Type folds in a Cordilleran Metamorphic

Core Complex (Raft River Mountains, northwestern Utah). *Tectonics, 6*, 423–448.
Mancktelow, N. S., & Pavlis, T. L. (1994). Fold-fault relationships in low-angle detachment systems. *Tectonics, 13*, 668–685.
Martínez-Martínez, J. M. (2006). Lateral interaction between metamorphic core complexes and less-extended, tilt-block domains: The Alpujarras strike-slip transfer fault zone (Betics, SE Spain). *Journal of Structural Geology, 28*, 602–620.
Martínez-Martínez, J. M., Soto, J. I., & Balanyá, J. C. (2002). Orthogonal folding of extensional detachments: Structure and origin of the Sierra Nevada elongated dome (Betics, SE Spain). *Tectonics, 21*, 1–20.
Martínez-Martínez, J. M., Soto, J. I., & Balanyá, J. C. (2004). Elongated domes in extended orogens: A mode of mountain uplift in the Betics (southeast Spain). *Geological Society of America Special Papers, 380*, 243–265.
Montanari, D., Corti, G., Sani, F., Del Ventisette, C., Bonini, M., & Moratti, G. (2010). Experimental investigation on granite emplacement during shortening. *Tectonophysics, 484*, 147–155.
Okay, Aİ. (1989). Tectonic units and sutures in the Pontides, northern Turkey. In A. M. C. Şengör (Ed.), *Tectonic evolution of the Tethyan Region* (pp. 109–115). Dordrecht: Kluwer.
Öner, Z., & Dilek, Y. (2011). Supradetachment basin evolution during continental extension: The Aegean province of western Anatolia, Turkey. *Geological Society of America Bulletin, 123*, 2115–2141.
Oyman, T., Özgenç, İ., Tokçaer, M., & Akbulut, M. (2013). Petrology, geochemistry, and evolution of the iron skarns along the northern contact of the Eğrigöz Plutonic Complex, Western Anatolia, Turkey. *Turkish Journal of Earth Sciences, 22*, 61–97.
Parsons, T., & Thompson, G. A. (1993). Does magmatism influence low-angle normal faulting? *Geology, 21*, 247–250.
Platt, J. P. (1980). Archaean greenstone belts: A structaral test of tectonic hypothesis. *Tectonophysics, 65*, 127–150.
Platt, J. P., Behr, W. M., & Cooper, F. J. (2015). Metamorphic core complexes: Windows into the mechanics and rheology of the crust. *Journal of the Geological Society, 172*, 9–27.
Ramberg, H. (1981). *Gravity, deformation and the Earth's crust: In theory, experiments and geological application*. New York, NY: Academic Press.
Rey, P. F., Teyssier, C., Kruckenberg, S. C., & Whitney, D. L. (2011). Viscous collision in channel explains double domes in metamorphic core complexes. *Geology, 39*, 387–390.
Ring, U., & Collins, A. S. (2005). U-Pb SIMS dating of synkinematic granites: timing of core-complex formation in the northern Anatolide belt of western Turkey. *Journal of the Geological Society, London, 162*, 289–298.
Ring, U., Laws, S., & Bernet, M. (1999). Structural analysis of a complex nappe sequence and late-orogenic basins from the Aegean Island of Samos, Greece. *Journal of Structural Geology, 21*, 1575–1601.
Ring, U. W. E., Johnson, C., Hetzel, R., & Gessner, K. (2003). Tectonic denudation of a Late CretaceousTertiary collisional belt: Regionally symmetric cooling patterns and their relation to extensional faults in the Anatolide belt of western Turkey. *Geological Magazine, 140*, 421–441.
Román-Berdiel, T. (1999). Geometry of granite emplacement in the upper crust: Contributions of analogue modelling. In *Understanding granites: Integrating new and classical techniques. Geological society, London, Special publication* (Vol. 168, pp. 77–94). London: The Geological Society of London.
Román-Berdiel, T., Aranguren, A., Cuevas, J., Tubía, J., Gapais, D., & Brun, J. (2000). Experiments on granite intrusion in transtension. In J. L. Vigneresse, Y. Mart, & B. Vendeville (Eds.), *Salt, Shale and Igneous Diapirs in and around Europe*, Geological Society, London, Special Publications (Vol. 174, pp. 21–42). London: The Geological Society of London.
Semiz, B., Ersoy, E. Y., Özpınar, Y., Helvacı, C., Palmer, M. R., & Billor, M. Z. (2015). 40Ar/39Ar geochronology, geochemistry and petrology of volcanic rocks from the Simav Graben, western Turkey. *Contributions to Mineralogy and Petrology, 170*, 24.
Singleton, J. S. (2012). Development of extension-parallel corrugations in the Buckskin-Rawhide metamorphic core complex, west-central Arizona. *Geological Society of America Bulletin, 125*, 453–472.
Teyssier, C., & Whitney, D. L. (2002). Gneiss domes and orogeny. *Geology, 30*, 1139–1142.
Thomson, S. N., & Ring, U. (2006). Thermochronologic evaluation of postcollision extension in the Anatolide orogen, western Turkey. *Tectonics, 25*, TC3005.
Uzel, B., Langereis, C. G., Kaymakçı, N., Sözbilir, H., Özkaymak, Ç., & Özkaptan, M. (2015). Paleomagnetic evidence for an inverse rotation history of Western Anatolia during the exhumation of Menderes core complex. *Earth and Planetary Science Letters, 414*, 108–125.
Verner, K., Žák, J., Šrámek, J., Paclíková, J., Zavřelová, A., Machek, M., & Johnson, K. (2014). Formation of elongated granite–migmatite domes as isostatic accommodation structures in collisional orogens. *Journal of Geodynamics, 73*, 100–117.
Vigneresse, J. L., & Clemens, J. D. (2000). Granitic magma ascent and emplacement: Neither diapirism nor neutral buoyancy. *Geological Society, London, Special Publications, 174*(1), 1–19.
Waldron, J. W. F. (2005). Extensional fault arrays in strike-slip and transtension. *Journal of Structural Geology, 27*, 23–34.
Wallace, R. E. (1951). Geometry of shearing stress and relation to faulting. *The Journal of Geology, 59*, 118–130.
Wernicke, B. (1981). Low-angle normal faults in the Basin and Range Province: Nappe tectonics in an extending orogen. *Nature, 291*, 645–648.
Wernicke, B., & Axen, G. J. (1988). On the role of isostasy in the evolution of normal fault systems. *Geology, 16*, 848–851.
Wernicke, B., Axen, G. J., & Snow, J. K. (1988). Basin and Range extensional tectonics at the latitude of Las Vegas, Nevada. *Geological Society of America Bulletin, 100*, 1738–1757.
Yılmaz, Y., Genç, Ş. C., Gürer, F., Bozcu, M., Yılmaz, K., Karacık, Z., … Elmas, A. (2000). When did western Anatolian grabens begin to develop? In E. Bozkurt, J. A. Winchester, & J. A. D. Piper (Eds.), *Tectonics and magmatism in Turkey and surrounding area* (Vol. 173, pp. 131–162). London: Geological Society, London, Special Publications.
Yin, A. (1991). Mechanisms for the formation of Domal and Basinal detachment faults: A three-dimensional analysis. *Journal of Geophysical Research: Solid Earth, 96*, 14577–14594.
Yin, A. (2004). Gneiss domes and gneiss dome systems. In D. L. Whitney, C. Teyssier, & C. S. Siddoway (Eds.), *Gneiss domes in orogeny* (Vol. 380, pp. 1–14). London: Geological Society of America Special Paper: Geological Society of America. doi:
Yin, A., Kapp, P. A., Murphy, M. A., Manning, C. E., Mark Harrison, T., Grove, M., … Cun-Ming, W. (1999). Significant late Neogene east-west extension in northern Tibet. *Geology, 27*, 787–790.